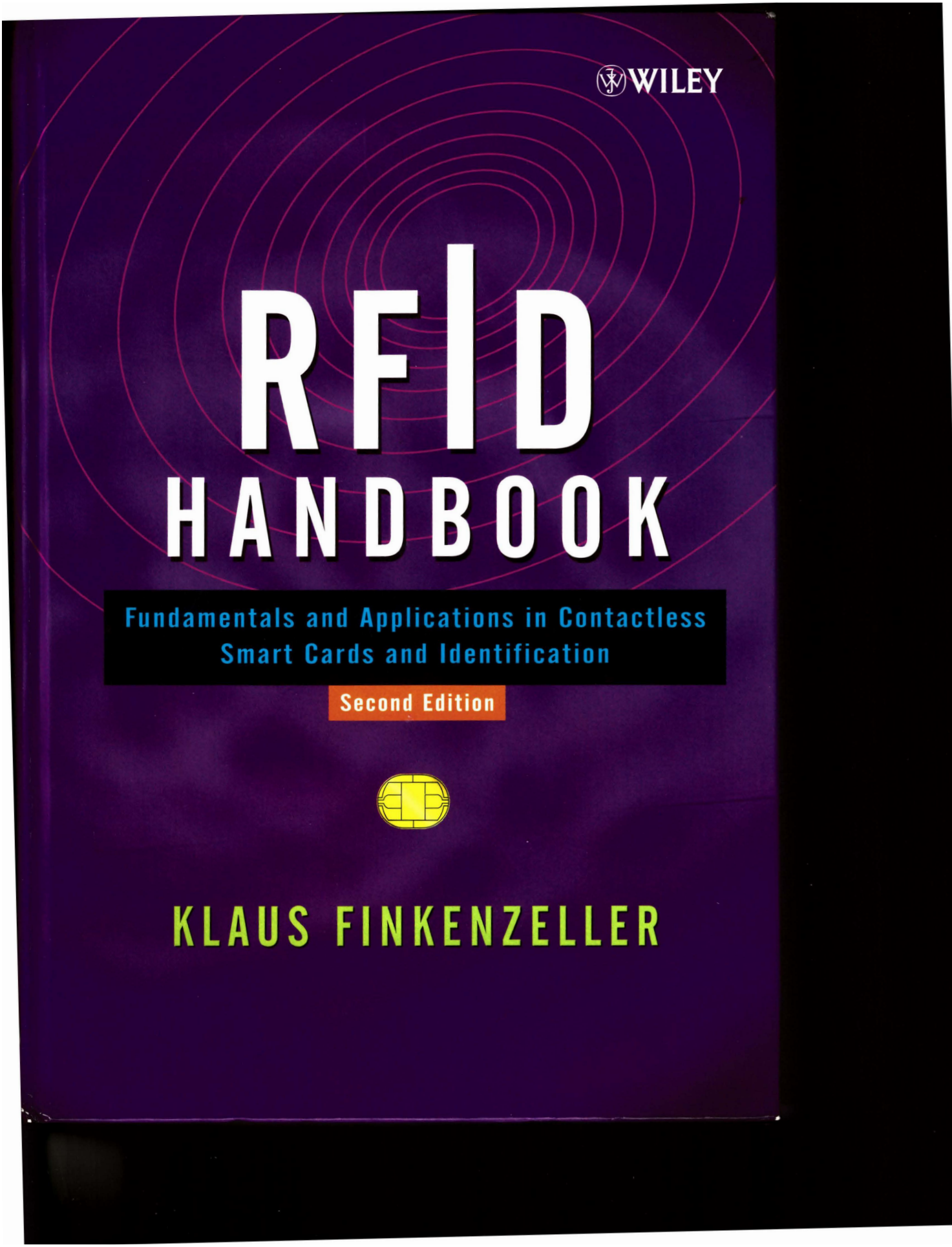


WAVELYNX EX. 1008, Pg. 1
WaveLynx Technologies v. ASSA Abloy, IPR2023-00730

First published under the title *RFID-Handbuch, 2 Auflage* by Carl Hanser Verlag
© Carl Hanser Verlag, Munich/FRG, 1999 All rights reserved
Authorized translation from the 2nd edition in the original German language
published by Carl Hanser Verlag, Munich/FRG

Copyright © 2003 John Wiley & Sons Ltd, The Atrium, Southern Gate, Chichester,
West Sussex PO19 8SQ, England

Telephone (+44) 1243 779777

Email (for orders and customer service enquiries): cs-books@wiley.co.uk
Visit our Home Page on www.wileyeurope.com or www.wiley.com

Reprinted September 2003, March and September 2004

All Rights Reserved. No part of this publication may be reproduced, stored in a retrieval system or transmitted in any form or by any means, electronic, mechanical, photocopying, recording, scanning or otherwise, except under the terms of the Copyright, Designs and Patents Act 1988 or under the terms of a licence issued by the Copyright Licensing Agency Ltd, 90 Tottenham Court Road, London W1T 4LP, UK, without the permission in writing of the Publisher. Requests to the Publisher should be addressed to the Permissions Department, John Wiley & Sons Ltd, The Atrium, Southern Gate, Chichester, West Sussex PO19 8SQ, England, or emailed to permreq@wiley.co.uk, or faxed to (+44) 1243 770620.

This publication is designed to provide accurate and authoritative information in regard to the subject matter covered. It is sold on the understanding that the Publisher is not engaged in rendering professional services. If professional advice or other expert assistance is required, the services of a competent professional should be sought.

Other Wiley Editorial Offices

John Wiley & Sons Inc., 111 River Street, Hoboken, NJ 07030, USA

Jossey-Bass, 989 Market Street, San Francisco, CA 94103-1741, USA

Wiley-VCH Verlag GmbH, Boschstr. 12, D-69469 Weinheim, Germany

John Wiley & Sons Australia Ltd, 33 Park Road, Milton, Queensland 4064, Australia

John Wiley & Sons (Asia) Pte Ltd, 2 Clementi Loop #02-01, Jin Xing Distripark, Singapore 129809

John Wiley & Sons Canada Ltd, 22 Worcester Road, Etobicoke, Ontario, Canada M9W 1L1

Wiley also publishes its books in a variety of electronic formats. Some content that appears in print may not be available in electronic books.

Library of Congress Cataloging-in-Publication Data

Finkenzeller, Klaus.
[RFID Handbuch. English]
RFID handbook : fundamentals and applications in contactless smart cards and identifcation/Klaus Finkenzeller; translated by Rachel Waddington. — 2nd ed.
p. cm.
Includes bibliographical references and index.
ISBN 0-470-84402-7 (alk. paper)
1. Inventory control — Automation. 2. Radio frequency identification systems. 3. Smart. cards. I. Title.

TS160.F5513 2003
658.7′87 — dc21

2002192439

British Library Cataloguing in Publication Data

A catalogue record for this book is available from the British Library

ISBN 0-470-84402-7

Typeset in 10/12pt Times by Laserwords Private Limited, Chennai, India
Printed and bound in Great Britain by Antony Rowe Ltd, Chippenham, Wiltshire
This book is printed on acid-free paper responsibly manufactured from sustainable forestry in which at least two trees are planted for each one used for paper production.

Conte

PREFACE
LIST OF ABBREVIATIC

1 Introduction
1.1 Automatic Ide
1.1.1 Barcod
1.1.2 Optical
1.1.3 Biometr
1.1.3.1
1.1.3.2
1.1.4 Smart c
1.1.4.1
1.1.4.2
1.1.5 RFID sy
1.2 A Comparisor
1.3 Components c

2 Differentiation
2.1 Fundamental [
2.2 Transponder C
2.2.1 Disks ar
2.2.2 Glass h
2.2.3 Plastic h
2.2.4 Tool an
2.2.5 Keys an
2.2.6 Clocks
2.2.7 ID-1 for
2.2.8 Smart la
2.2.9 Coil-on-
2.2.10 Other fo
2.3 Frequency, Ra
2.4 Information Pr
2.4.1 Low-end
2.4.2 Mid-ran
2.4.3 High-en
2.5 Selection Criter
2.5.1 Operatir
2.5.2 Range



WAVELYNX EX. 1008, Pg. 2
WaveLynx Technologies v. ASSA Abloy, IPR2023-00730

Preface to the 2nd Edition

This book is aimed at an extremely wide range of readers. First and foremost it is intended for students and engineers who find themselves confronted with RFID technology for the first time. A few basic chapters are provided for this audience describing the functionality of RFID technology and the physical and IT-related principles underlying this field. The book is also intended for practitioners who, as users, wish to or need to obtain as comprehensive and detailed an overview of the various technologies, the legal framework or the possible applications of RFID as possible.

Although a wide range of individual articles are now available on this subject, the task of gathering all this scattered information together when it is needed is a tiresome and time-consuming one — as researching this book has proved. This book therefore aims to fill a gap in the range of literature on the subject of RFID. The need for well-founded technical literature in this field is proven by the fortunate fact that this book has now also appeared in Chinese and Japanese translation. Further information on the German version of the RFID handbook and the translations can be found on the homepage of this book, http://RFID-handbook.com.

This book uses numerous pictures and diagrams to attempt to give a graphic representation of RFID technology in the truest sense of the word. Particular emphasis is placed on the physical principles of RFID, which is why the chapter on this subject is by far the most comprehensive of the book. However, practical considerations are also assigned great importance. For this reason the chapter entitled 'Example Applications' is also particularly comprehensive.

Technological developments in the field of RFID technology are proceeding at such a pace that although a book like this can explain the general scientific principles it is not dynamic enough to be able to explore the latest trends regarding the most recent products on the market and the latest standards and regulations. I am therefore grateful for any suggestions and advice — particularly from the field of industry. The basic concepts and underlying physical principles remain, however, and provide a good background for understanding the latest developments.

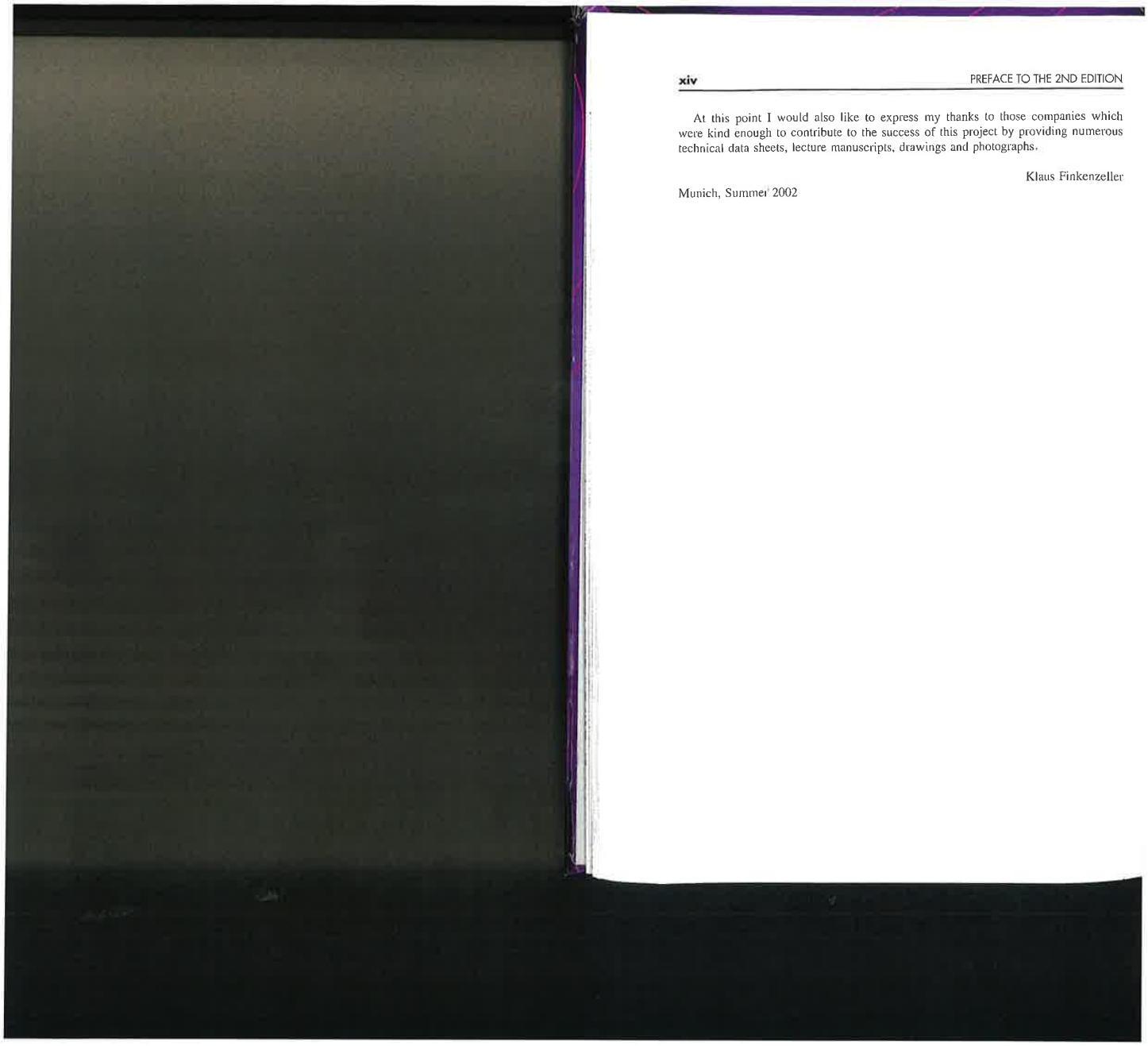
Unfortunately, the market overview that was previously included has had to be omitted from the 2nd edition of the book, as the growing number of providers has made it increasingly difficult to retain an overview of the numerous transponders available on the market. However, a detailed introduction to the physical principles of UHF and microwave systems (Section 4.2), which will become increasingly important in Europe with the approval of the corresponding frequency ranges in the 868 MHz band, has been added. The chapter on standardisation has been extended in order to keep up with the rapid development in this field.

WAVELYNX EX. 1008, Pg. 3
WaveLynx Technologies v. ASSA Abloy, IPR2023-00730

At this point I would also like to express my thanks to those companies which were kind enough to contribute to the success of this project by providing numerous technical data sheets, lecture manuscripts, drawings and photographs.

Klaus Finkenzeller

Munich, Summer 2002



WAVELYNX EX. 1008, Pg. 4
WaveLynx Technologies v. ASSA Abloy, IPR2023-00730

Table 1.1 Comparison of different RFID systems showing their advantages and disadvantages

System parameters	Barcode	OCR	Voice recog.	Biometry	Smart card	RFID systems
Typical data quantity (bytes)	1–100	1–100	—	—	16–64 k	16–64 k
Data density	Low	Low	High	High	Very high	Very high
Machine readability	Good	Good	Expensive	Expensive	Good	Good
Readability by people	Limited	Simple	Simple	Difficult	Impossible	Impossible
Influence of dirt/damp	Very high	Very high	—	—	Possible (contacts)	No influence
Influence of (opt.) covering	Total failure	Total failure	—	Possible	—	No influence
Influence of direction and position	Low	Low	—	—	Unidirectional	No influence
Degradation/wear	Limited	Limited	—	—	Contacts	No influence
Purchase cost/reading electronics	Very low	Medium	Very high	Very high	Low	Medium
Operating costs (e.g. printer)	Low	Low	None	None	Medium (contacts)	None
Unauthorised copying/modification	Slight	Slight	Possible* (audio tape)	Impossible	Impossible	Impossible
Reading speed (including handling of data carrier)	Low ~4 s	Low ~3 s	Very low >5 s	Very low >5–10 s	Low ~4 s	Very fast ~0.5 s
Maximum distance between data carrier and reader	0–50 cm	<1 cm Scanner	0–50 cm	Direct contact**	Direct contact	0–5-m, microwave

*The danger of 'Replay' can be reduced by selecting the text to be spoken using a random generator, because the text that must be spoken is not known in advance.
**This only applies for fingerprint ID. In the case of retina or iris evaluation direct contact is not necessary or possible.

WAVELYNX EX. 1008, Pg. 5
WaveLynx Technologies v. ASSA Abloy, IPR2023-00730

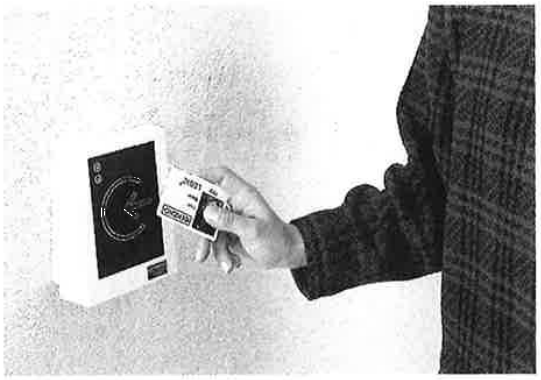


Figure 1.8 RFID reader and contactless smart card in practical use (reproduced by permission of Kaba Benzing GmbH)

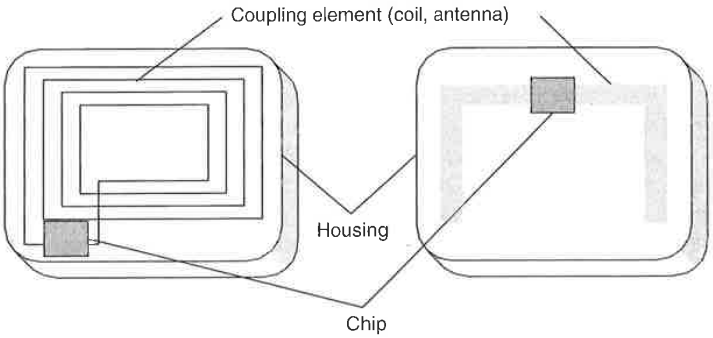


Figure 1.9 Basic layout of the RFID data-carrying device, the transponder. Left, inductively coupled transponder with antenna coil; right, microwave transponder with dipolar antenna

When the transponder, which does not usually possess its own voltage supply (battery), is not within the interrogation zone of a reader it is totally passive. The transponder is only activated when it is within the interrogation zone of a reader. The power required to activate the transponder is supplied to the transponder through the coupling unit (contactless), as are the timing pulse and data.

WAVELYNX EX. 1008, Pg. 6
WaveLynx Technologies v. ASSA Abloy, IPR2023-00730

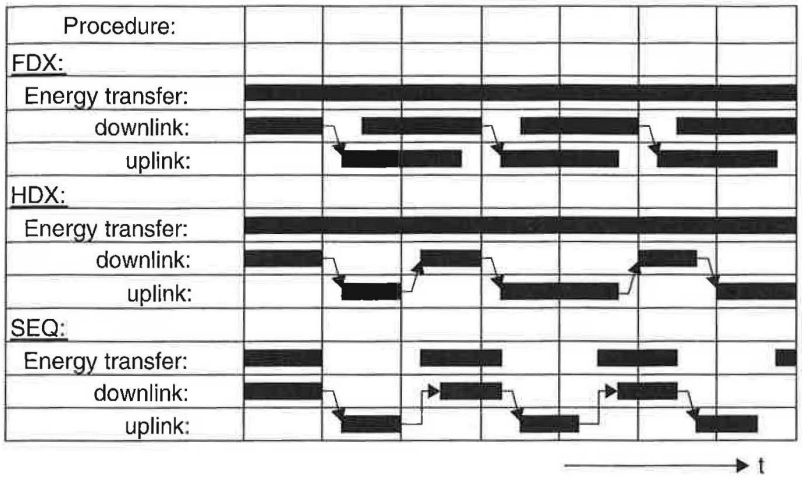


Figure 3.12 Representation of full duplex, half duplex and sequential systems over time. Data transfer from the reader to the transponder is termed downlink, while data transfer from the transponder to the reader is termed uplink

operation → *pulsed system*). Data transfer from the transponder to the reader occurs in the pauses between the power supply to the transponder. See Figure 3.12 for a representation of full duplex, half duplex and sequential systems.

Unfortunately, the literature relating to RFID has not yet been able to agree a consistent nomenclature for these system variants. Rather, there has been a confusing and inconsistent classification of individual systems into full and half duplex procedures. Thus pulsed systems are often termed half duplex systems — this is correct from the point of view of data transfer — and all unpulsed systems are falsely classified as full duplex systems. For this reason, in this book pulsed systems — for differentiation from other procedures, and unlike most RFID literature(!) — are termed sequential systems (SEQ).

3.2.1 Inductive coupling

3.2.1.1 Power supply to passive transponders

An inductively coupled transponder comprises an electronic data-carrying device, usually a single microchip, and a large area coil that functions as an antenna.

Inductively coupled transponders are almost always operated passively. This means that all the energy needed for the operation of the microchip has to be provided by the reader (Figure 3.13). For this purpose, the reader's antenna coil generates a strong, high frequency electromagnetic field, which penetrates the cross-section of the coil area and the area around the coil. Because the wavelength of the frequency range used (<135 kHz: 2400 m, 13.56 MHz: 22.1 m) is several times greater than the distance between the reader's antenna and the transponder, the electromagnetic field may be treated as a simple magnetic alternating field with regard to the distance between transponder and antenna (see Section 4.2.1.1 for further details).

WAVELYNX EX. 1008, Pg. 7
WaveLynx Technologies v. ASSA Abloy, IPR2023-00730

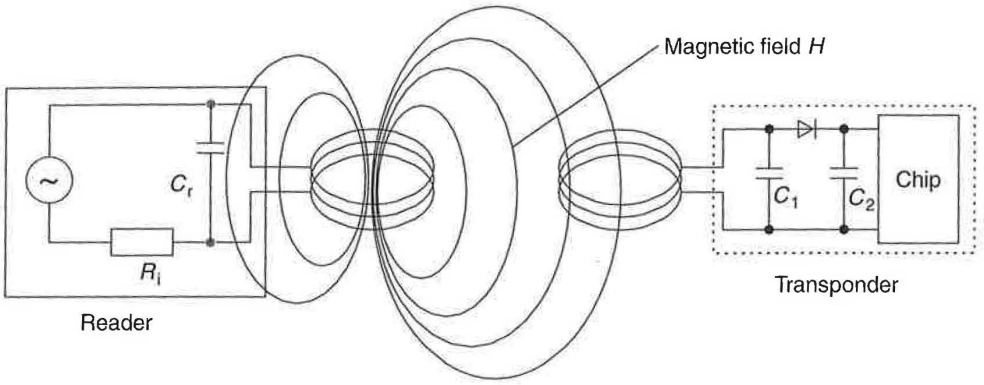


Figure 3.13 Power supply to an inductively coupled transponder from the energy of the magnetic alternating field generated by the reader

A small part of the emitted field penetrates the antenna coil of the transponder, which is some distance away from the coil of the reader. A voltage U_i is generated in the transponder's antenna coil by inductance. This voltage is rectified and serves as the power supply for the data-carrying device (microchip). A capacitor C_r is connected in parallel with the reader's antenna coil, the capacitance of this capacitor being selected such that it works with the coil inductance of the antenna coil to form a parallel resonant circuit with a resonant frequency that corresponds with the transmission frequency of the reader. Very high currents are generated in the antenna coil of the reader by resonance step-up in the parallel resonant circuit, which can be used to generate the required field strengths for the operation of the remote transponder.

The antenna coil of the transponder and the capacitor C_1 form a resonant circuit tuned to the transmission frequency of the reader. The voltage U at the transponder coil reaches a maximum due to resonance step-up in the parallel resonant circuit.

The layout of the two coils can also be interpreted as a transformer (*transformer coupling*), in which case there is only a very weak coupling between the two windings (Figure 3.14). The efficiency of power transfer between the antenna coil of the reader and the transponder is proportional to the operating frequency f, the number of windings n, the area A enclosed by the transponder coil, the angle of the two coils relative to each other and the distance between the two coils.

As frequency f increases, the required coil inductance of the transponder coil, and thus the number of windings n decreases (135 kHz: typical 100–1000 windings, 13.56 MHz: typical 3–10 windings). Because the voltage induced in the transponder is still proportional to frequency f (see Chapter 4), the reduced number of windings barely affects the efficiency of power transfer at higher frequencies. Figure 3.15 shows a reader for an inductively coupled transponder.

3.2.1.2 Data transfer transponder → reader

Load modulation As described above, inductively coupled systems are based upon a *transformer-type coupling* between the primary coil in the reader and the secondary coil in the transponder. This is true when the distance between the coils does not exceed

WAVELYNX EX. 1008, Pg. 8
WaveLynx Technologies v. ASSA Abloy, IPR2023-00730

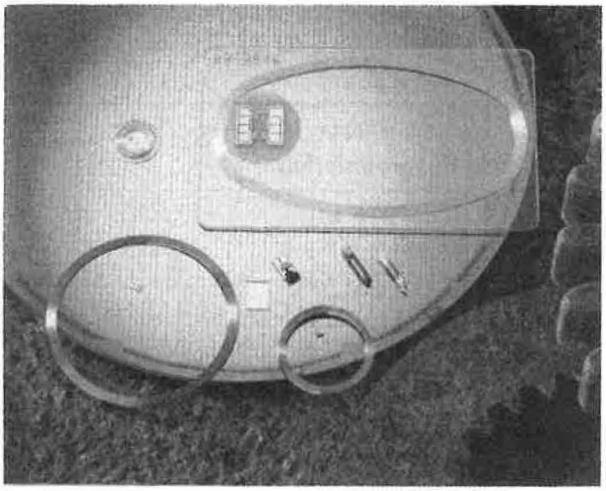


Figure 3.14 Different designs of inductively coupled transponders. The photo shows half finished transponders, i.e. transponders before injection into a plastic housing (reproduced by permission of AmaTech GmbH & Co. KG, D-Pfronten)

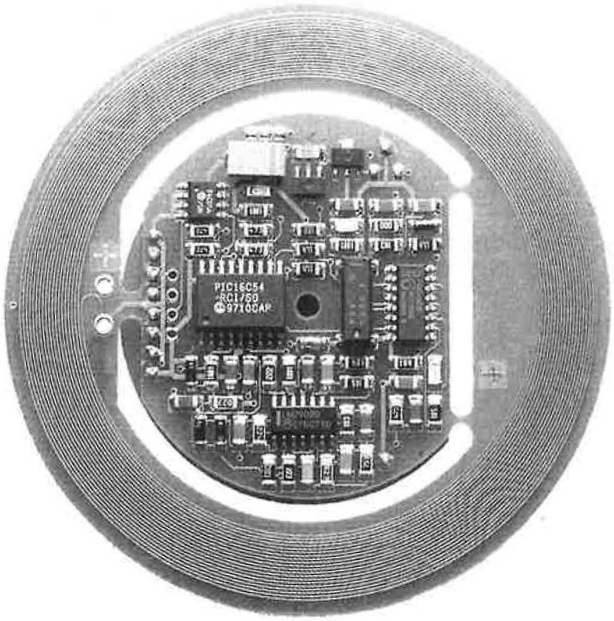


Figure 3.15 Reader for inductively coupled transponder in the frequency range <135 kHz with integral antenna (reproduced by permission of easy-key System, micron, Halbergmoos)

0.16 λ, so that the transponder is located in the *near field* of the transmitter antenna (for a more detailed definition of the near and far fields, please refer to Chapter 4).

If a resonant transponder (i.e. a transponder with a self-resonant frequency corresponding with the transmission frequency of the reader) is placed within the magnetic alternating field of the reader's antenna, the transponder draws energy from the magnetic field. The resulting feedback of the transponder on the reader's antenna can be

WAVELYNX EX. 1008, Pg. 9
WaveLynx Technologies v. ASSA Abloy, IPR2023-00730

Table 3.6 Overview of the power consumption of various RFID-ASIC building blocks (Atmel, 1994). The minimum supply voltage required for the operation of the microchip is 1.8 V, the maximum permissible voltage is 10 V

	Memory (Bytes)	Write/read distance	Power consumption	Frequency	Application
ASIC#1	6	15 cm	10 µA	120 kHz	Animal ID
ASIC#2	32	13 cm	600 µA	120 kHz	Goods flow, access check
ASIC#3	256	2 cm	6 µA	128 kHz	Public transport
ASIC#4	256	0.5 cm	<1 mA	4 MHz*	Goods flow, public transport
ASIC#5	256	<2 cm	~1 mA	4/13.56 MHz	Goods flow
ASIC#6	256	100 cm	500 µA	125 kHz	Access check
ASIC#7	2048	0.3 cm	<10 mA	4.91 MHz*	Contactless chip cards
ASIC#8	1024	10 cm	~1 mA	13.56 MHz	Public transport
ASIC#9	8	100 cm	<1 mA	125 kHz	Goods flow
ASIC#10	128	100 cm	<1 mA	125 kHz	Access check

*Close coupling system.

represented as *transformed impedance* Z_T in the antenna coil of the reader. Switching a *load resistor* on and off at the transponder's antenna therefore brings about a change in the impedance Z_T, and thus voltage changes at the reader's antenna (see Section 4.1.10.3). This has the effect of an amplitude modulation of the voltage U_L at the reader's antenna coil by the remote transponder. If the timing with which the load resistor is switched on and off is controlled by data, this data can be transferred from the transponder to the reader. This type of data transfer is called *load modulation*.

To reclaim the data at the reader, the voltage tapped at the reader's antenna is rectified. This represents the demodulation of an amplitude modulated signal. An example circuit is shown in Section 11.3.

Load modulation with subcarrier Due to the weak coupling between the reader antenna and the transponder antenna, the voltage fluctuations at the antenna of the reader that represent the useful signal are smaller by orders of magnitude than the output voltage of the reader.

In practice, for a 13.56 MHz system, given an antenna voltage of approximately 100 V (voltage step-up by resonance) a useful signal of around 10 mV can be expected (=80 dB signal/noise ratio). Because detecting this slight voltage change requires highly complicated circuitry, the modulation sidebands created by the amplitude modulation of the antenna voltage are utilised (Figure 3.16).

If the additional load resistor in the transponder is switched on and off at a very high elementary frequency f_S, then two spectral lines are created at a distance of $\pm f_S$ around the transmission frequency of the reader f_{READER}, and these can be easily detected (however f_S must be less than f_{READER}). In the terminology of radio technology the new elementary frequency is called a *subcarrier*). Data transfer is by ASK, FSK or PSK modulation of the subcarrier in time with the data flow. This represents an amplitude modulation of the subcarrier.

Load modulation with a subcarrier creates two modulation sidebands at the reader's antenna at the distance of the subcarrier frequency around the operating frequency f_{READER} (Figure 3.17). These modulation sidebands can be separated from

WAVELYNX EX. 1008, Pg. 10
WaveLynx Technologies v. ASSA Abloy, IPR2023-00730

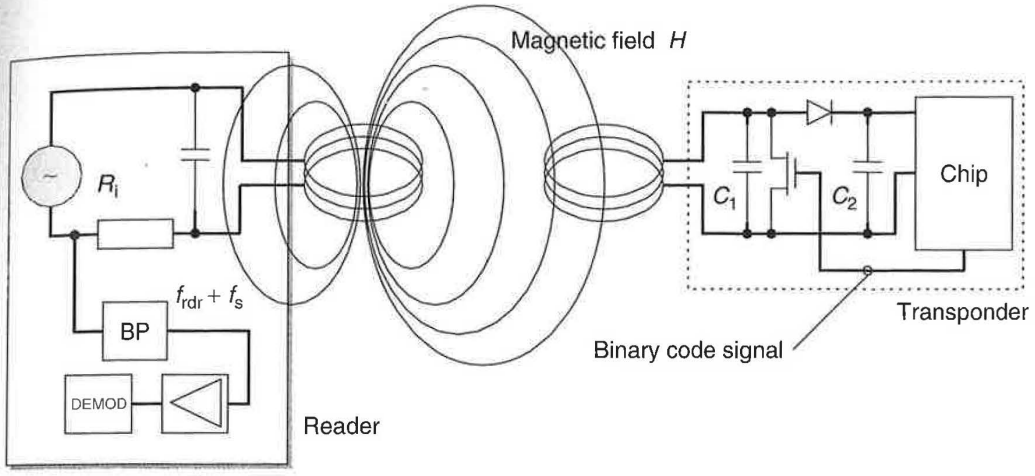


Figure 3.16 Generation of load modulation in the transponder by switching the drain-source resistance of an FET on the chip. The reader illustrated is designed for the detection of a subcarrier

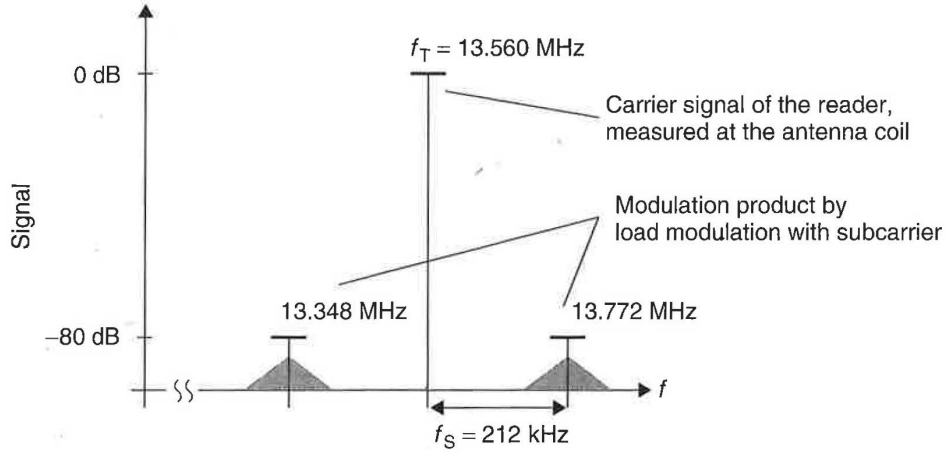


Figure 3.17 Load modulation creates two sidebands at a distance of the subcarrier frequency f_S around the transmission frequency of the reader. The actual information is carried in the sidebands of the two subcarrier sidebands, which are themselves created by the modulation of the subcarrier

the significantly stronger signal of the reader by bandpass (BP) filtering on one of the two frequencies $f_{READER} \pm f_S$. Once it has been amplified, the subcarrier signal is now very simple to demodulate.

Because of the large bandwidth required for the transmission of a subcarrier, this procedure can only be used in the ISM frequency ranges for which this is permitted, 6.78 MHz, 13.56 MHz and 27.125 MHz (see also Chapter 5).

Example circuit–load modulation with subcarrier Figure 3.18 shows an example circuit for a transponder using load modulation with a subcarrier. The circuit is designed for an operating frequency of 13.56 MHz and generates a subcarrier of 212 kHz.

WAVELYNX EX. 1008, Pg. 11
WaveLynx Technologies v. ASSA Abloy, IPR2023-00730

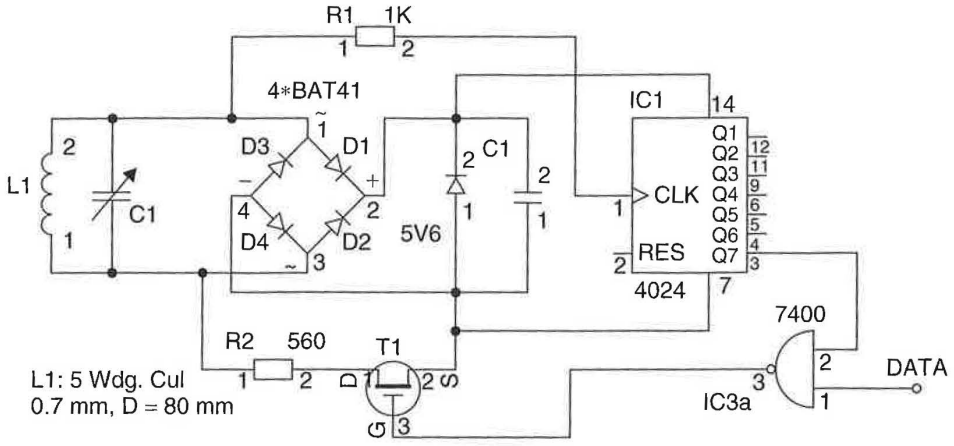


Figure 3.18 Example circuit for the generation of load modulation with subcarrier in an inductively coupled transponder

The voltage induced at the antenna coil L1 by the magnetic alternating field of the reader is rectified using the bridge rectifier (D1–D4) and after additional smoothing (C1) is available to the circuit as supply voltage. The parallel regulator (ZD 5V6) prevents the supply voltage from being subject to an uncontrolled increase when the transponder approaches the reader antenna.

Part of the high frequency antenna voltage (13.56 MHz) travels to the frequency divider's timing input (CLK) via the protective resistor (R1) and provides the transponder with the basis for the generation of an internal clocking signal. After division by $2^6 (= 64)$ a subcarrier clocking signal of 212 kHz is available at output Q7. The subcarrier clocking signal, controlled by a serial data flow at the data input (DATA), is passed to the switch (T1). If there is a logical HIGH signal at the data input (DATA), then the subcarrier clocking signal is passed to the switch (T1). The load resistor (R2) is then switched on and off in time with the subcarrier frequency.

Optionally in the depicted circuit the transponder resonant circuit can be brought into resonance with the capacitor C1 at 13.56 MHz. The range of this 'minimal transponder' can be significantly increased in this manner.

Subharmonic procedure The subharmonic of a sinusoidal voltage A with a defined frequency f_A is a sinusoidal voltage B, whose frequency f_B is derived from an integer division of the frequency f_A. The subharmonics of the frequency f_A are therefore the frequencies $f_A/2$, $f_A/3$, $f_A/4 \ldots$.

In the subharmonic transfer procedure, a second frequency f_B, which is usually lower by a factor of two, is derived by digital division by two of the reader's transmission frequency f_A. The output signal f_B of a binary divider can now be modulated with the data stream from the transponder. The modulated signal is then fed back into the transponder's antenna via an output driver.

One popular operating frequency for subharmonic systems is 128 kHz. This gives rise to a transponder response frequency of 64 kHz.

The transponder's antenna consists of a coil with a central tap, whereby the power supply is taken from one end. The transponder's return signal is fed into the coil's second connection (Figure 3.19).

WAVELYNX EX. 1008, Pg. 12
WaveLynx Technologies v. ASSA Abloy, IPR2023-00730

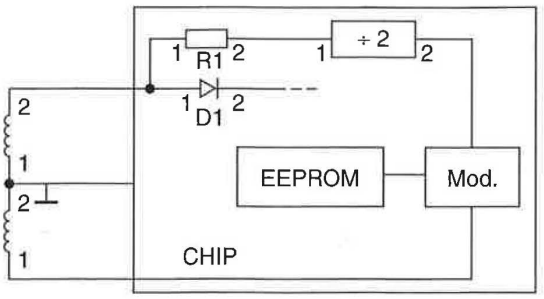


Figure 3.19 Basic circuit of a transponder with subharmonic back frequency. The received clocking signal is split into two, the data is modulated and fed into the transponder coil via a tap

3.2.2 Electromagnetic backscatter coupling

3.2.2.1 Power supply to the transponder

RFID systems in which the gap between reader and transponder is greater than 1 m are called *long-range systems*. These systems are operated at the *UHF frequencies* of 868 MHz (Europe) and 915 MHz (USA), and at the *microwave frequencies* 2.5 GHz and 5.8 GHz. The short wavelengths of these frequency ranges facilitate the construction of antennas with far smaller dimensions and greater efficiency than would be possible using frequency ranges below 30 MHz.

In order to be able to assess the energy available for the operation of a transponder we first calculate the *free space path loss* a_F in relation to the distance r between the transponder and the reader's antenna, the gain G_T and G_R of the transponder's and reader's antenna, plus the transmission frequency f of the reader:

$$a_F = -147.6 + 20\log(r) + 20\log(f) - 10\log(G_T) - 10\log(G_R) \qquad (3.1)$$

The free space path loss is a measure of the relationship between the HF power emitted by a reader into 'free space' and the HF power received by the transponder.

Using current low power semiconductor technology, transponder chips can be produced with a power consumption of no more than 5 μW (Friedrich and Annala, 2001). The efficiency of an integrated rectifier can be assumed to be 5–25% in the UHF and microwave range (Tanneberger, 1995). Given an efficiency of 10%, we thus require received power of $P_e = 50\,\mu W$ at the terminal of the transponder antenna for the operation of the transponder chip. This means that where the reader's transmission power is $P_s = 0.5$ W EIRP (effective isotropic radiated power) the free space path loss may not exceed 40 dB ($P_s/P_e = 10\,000/1$) if sufficiently high power is to be obtained at the transponder antenna for the operation of the transponder. A glance at Table 3.7 shows that at a transmission frequency of 868 MHz a *range* of a little over 3 m would be realisable; at 2.45 GHz a little over 1 m could be achieved. If the transponder's chip had a greater power consumption the achievable range would fall accordingly.

In order to achieve long ranges of up to 15 m or to be able to operate transponder chips with a greater power consumption at an acceptable range, backscatter transponders often have a backup battery to supply power to the transponder chip (Figure 3.20). To prevent this battery from being loaded unnecessarily, the microchips generally have

WAVELYNX EX. 1008, Pg. 13
WaveLynx Technologies v. ASSA Abloy, IPR2023-00730

4

Physical Principles of RFID Systems

The vast majority of RFID systems operate according to the principle of *inductive coupling*. Therefore, understanding of the procedures of power and data transfer requires a thorough grounding in the physical principles of magnetic phenomena. This chapter therefore contains a particularly intensive study of the theory of magnetic fields from the point of view of RFID.

Electromagnetic fields — radio waves in the classic sense — are used in RFID systems that operate at above 30 MHz. To aid understanding of these systems we will investigate the propagation of waves in the far field and the principles of radar technology.

Electric fields play a secondary role and are only exploited for capacitive data transmission in close coupling systems. Therefore, this type of field will not be discussed further.

4.1 Magnetic Field

4.1.1 Magnetic field strength *H*

Every moving charge (electrons in wires or in a vacuum), i.e. flow of current, is associated with a *magnetic field* (Figure 4.1). The intensity of the magnetic field can be demonstrated experimentally by the forces acting on a magnetic needle (compass) or a second electric current. The magnitude of the magnetic field is described by the *magnetic field strength* H regardless of the material properties of the space.

In the general form we can say that: 'the contour integral of magnetic field strength along a closed curve is equal to the sum of the current strengths of the currents within it' (Kuchling, 1985).

$$\sum I = \oint \vec{H} \cdot \vec{ds} \tag{4.1}$$

We can use this formula to calculate the field strength H for different types of conductor. See Figure 4.2.

RFID Handbook: Fundamentals and Applications in Contactless Smart Cards and Identification. Klaus Finkenzeller
© 2003 John Wiley & Sons, Ltd ISBN: 0-470-84402-7

WAVELYNX EX. 1008, Pg. 14
WaveLynx Technologies v. ASSA Abloy, IPR2023-00730

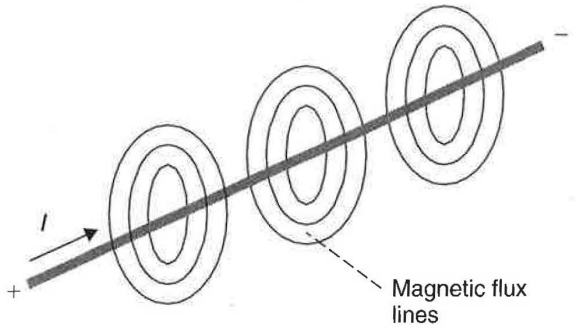


Figure 4.1 Lines of magnetic flux are generated around every current-carrying conductor

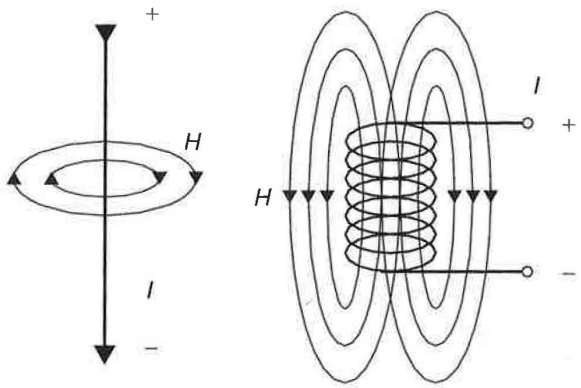


Figure 4.2 Lines of magnetic flux around a current-carrying conductor and a current-carrying cylindrical coil

Table 4.1 Constants used

Constant	Symbol	Value and unit
Electric field constant	ε_0	8.85×10^{-12} As/Vm
Magnetic field constant	μ_0	1.257×10^{-6} Vs/Am
Speed of light	c	299 792 km/s
Boltzmann constant	k	$1.380\,662 \times 10^{-23}$ J/K

In a straight conductor the field strength H along a circular *flux line* at a distance r is constant. The following is true (Kuchling, 1985):

$$H = \frac{1}{2\pi r} \tag{4.2}$$

4.1.1.1 Path of field strength H(x) in conductor loops

So-called 'short cylindrical coils' or conductor loops are used as magnetic antennas to generate the *magnetic alternating field* in the write/read devices of inductively coupled RFID systems (Figure 4.3).

WAVELYNX EX. 1008, Pg. 15
WaveLynx Technologies v. ASSA Abloy, IPR2023-00730

Table 4.2 Units and abbreviations used

Variable	Symbol	Unit	Abbreviation
Magnetic field strength	H	Ampere per meter	A/m
Magnetic flux (n = number of windings)	Φ	Volt seconds	Vs
	$\Psi = n\Phi$		
Magnetic inductance	B	Volt seconds per meter squared	Vs/m^2
Inductance	L	Henry	H
Mutual inductance	M	Henry	H
Electric field strength	E	Volts per metre	V/m
Electric current	I	Ampere	A
Electric voltage	U	Volt	V
Capacitance	C	Farad	F
Frequency	f	Hertz	Hz
Angular frequency	$\omega = 2\pi f$	1/seconds	1/s
Length	l	Metre	m
Area	A	Metre squared	m^2
Speed	v	Metres per second	m/s
Impedance	Z	Ohm	Ω
Wavelength	λ	Metre	m
Power	P	Watt	W
Power density	S	Watts per metre squared	W/m^2

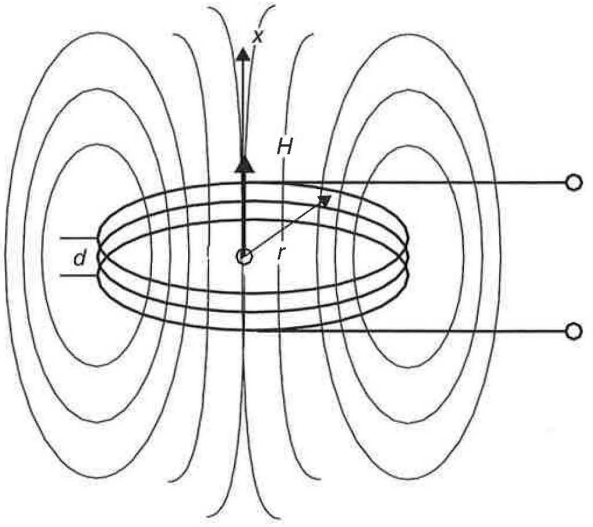


Figure 4.3 The path of the lines of magnetic flux around a short cylindrical coil, or conductor loop, similar to those employed in the transmitter antennas of inductively coupled RFID systems

If the measuring point is moved away from the centre of the coil along the coil axis (x axis), then the strength of the field H will decrease as the distance x is increased. A more in-depth investigation shows that the field strength in relation to the radius (or area) of the coil remains constant up to a certain distance and then falls rapidly (see Figure 4.4). In free space, the decay of field strength is approximately 60 dB per

WAVELYNX EX. 1008, Pg. 16
WaveLynx Technologies v. ASSA Abloy, IPR2023-00730

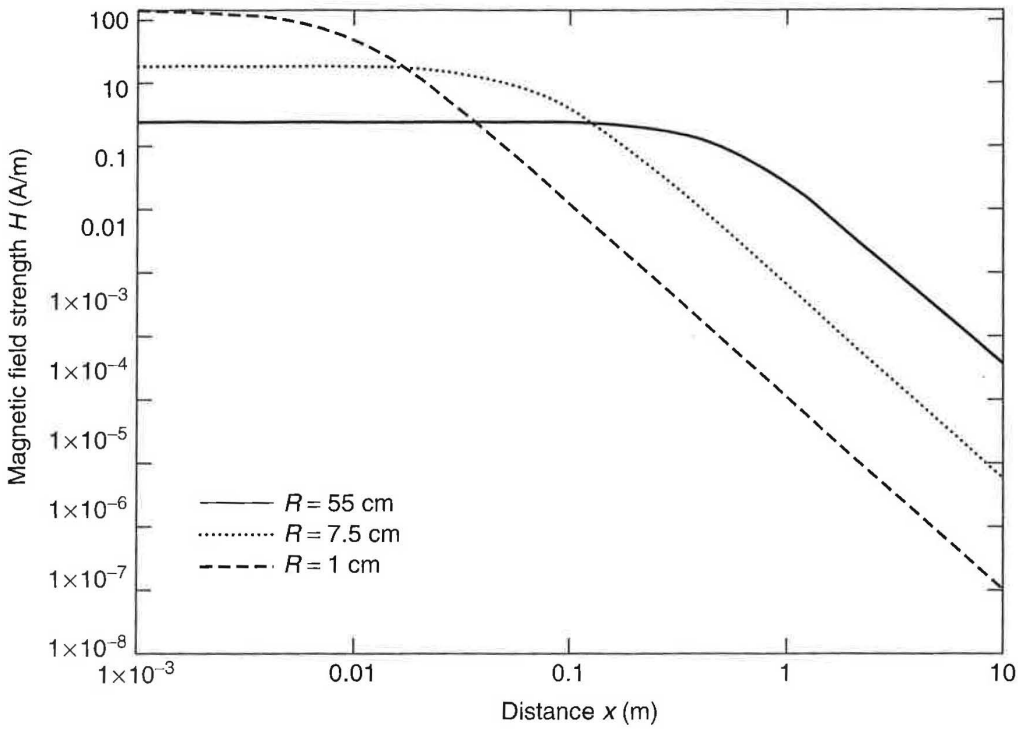


Figure 4.4 Path of magnetic field strength H in the near field of short cylinder coils, or conductor coils, as the distance in the x direction is increased

decade in the near field of the coil, and flattens out to 20 dB per decade in the far field of the electromagnetic wave that is generated (a more precise explanation of these effects can be found in Section 4.2.1).

The following equation can be used to calculate the path of field strength along the x axis of a round coil (= conductor loop) similar to those employed in the transmitter antennas of inductively coupled RFID systems (Paul, 1993):

$$H = \frac{I \cdot N \cdot R^2}{2\sqrt{(R^2 + x^2)^3}} \tag{4.3}$$

where N is the number of windings, R is the circle radius r and x is the distance from the centre of the coil in the x direction. The following boundary condition applies to this equation: $d \ll R$ and $x < \lambda/2\pi$ (the transition into the electromagnetic far field begins at a distance $>2\pi$; see Section 4.2.1).

At distance 0 or, in other words, at the centre of the antenna, the formula can be simplified to (Kuchling, 1985):

$$H = \frac{I \cdot N}{2R} \tag{4.4}$$

We can calculate the *field strength path* of a rectangular conductor loop with edge length $a \times b$ at a distance of x using the following equation. This format is often used

WAVELYNX EX. 1008, Pg. 17
WaveLynx Technologies v. ASSA Abloy, IPR2023-00730

as a transmitter antenna.

$$H = \frac{N \cdot I \cdot ab}{4\pi\sqrt{\left(\frac{a}{2}\right)^2 + \left(\frac{b}{2}\right)^2 + x^2}} \cdot \left(\frac{1}{\left(\frac{a}{2}\right)^2 + x^2} + \frac{1}{\left(\frac{b}{2}\right)^2 + x^2} \right) \tag{4.5}$$

Figure 4.4 shows the calculated field strength path $H(x)$ for three different antennas at a distance 0–20 m. The number of windings and the antenna current are constant in each case; the antennas differ only in radius R. The calculation is based upon the following values: $H1$: $R = 55$ cm, $H2$: $R = 7.5$ cm, $H3$: $R = 1$ cm.

The calculation results confirm that the increase in field strength flattens out at short distances ($x < R$) from the antenna coil. Interestingly, the smallest antenna exhibits a significantly higher field strength at the centre of the antenna (distance = 0), but at greater distances ($x > R$) the largest antenna generates a significantly higher field strength. It is vital that this effect is taken into account in the design of antennas for inductively coupled RFID systems.

4.1.1.2 Optimal antenna diameter

If the radius R of the transmitter antenna is varied at a constant distance x from the transmitter antenna under the simplifying assumption of constant coil current I in the transmitter antenna, then field strength H is found to be at its highest at a certain ratio of distance x to antenna radius R. This means that for every *read range* of an RFID system there is an optimal antenna radius R. This is quickly illustrated by a glance at Figure 4.4: if the selected antenna radius is too great, the field strength is too low even at a distance $x = 0$ from the transmission antenna. If, on the other hand, the selected antenna radius is too small, then we find ourselves within the range in which the field strength falls in proportion to x^3.

Figure 4.5 shows the graph of field strength H as the coil radius R is varied. The optimal coil radius for different read ranges is always the maximum point of the graph $H(R)$. To find the mathematical relationship between the maximum field strength H and the coil radius R we must first find the inflection point of the function $H(R)$ (see equation 4.3) (Lee, 1999). To do this we find the first derivative $H'(R)$ by differentiating $H(R)$ with respect to R:

$$H'(R) = \frac{\mathrm{d}}{\mathrm{d}R} H(R) = \frac{2 \cdot I \cdot N \cdot R}{\sqrt{(R^2 + x^2)^3}} - \frac{3 \cdot I \cdot N \cdot R^3}{(R^2 + x^2) \cdot \sqrt{(R^2 + x^2)^3}} \tag{4.6}$$

The inflection point, and thus the maximum value of the function $H(R)$, is found from the following zero points of the derivative $H'(R)$:

$$R_1 = x \cdot \sqrt{2}; \qquad R_2 = -x \cdot \sqrt{2} \tag{4.7}$$

WAVELYNX EX. 1008, Pg. 18
WaveLynx Technologies v. ASSA Abloy, IPR2023-00730

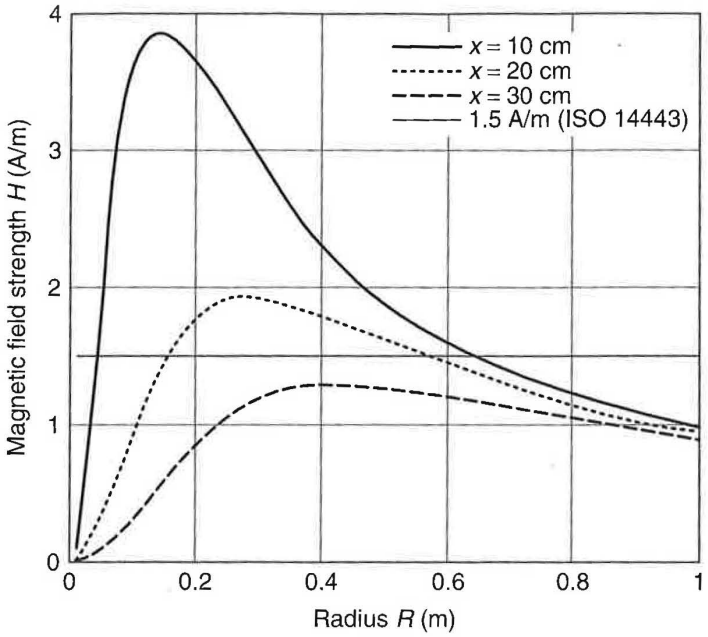


Figure 4.5 Field strength H of a transmission antenna given a constant distance x and variable radius R, where $I = 1$ A and $N = 1$

The optimal radius of a transmission antenna is thus twice the maximum desired read range. The second zero point is negative merely because the magnetic field H of a conductor loop propagates in both directions of the x axis (see also Figure 4.3).

However, an accurate assessment of a system's maximum read range requires knowledge of the *interrogation field strength* H_{min} of the transponder in question (see Section 4.1.9). If the selected antenna radius is too great, then there is the danger that the field strength H may be too low to supply the transponder with sufficient operating energy, even at a distance $x = 0$.

4.1.2 Magnetic flux and magnetic flux density

The magnetic field of a (cylindrical) coil will exert a force on a magnetic needle. If a soft iron core is inserted into a (cylindrical) coil — all other things remaining equal — then the force acting on the magnetic needle will increase. The quotient $I \times N$ (Section 4.1.1) remains constant and therefore so does field strength. However, the flux density — the total number of flux lines — which is decisive for the force generated (cf. Pauls, 1993), has increased.

The total number of lines of magnetic flux that pass through the inside of a cylindrical coil, for example, is denoted by *magnetic flux* Φ. Magnetic flux density B is a further variable related to area A (this variable is often referred to as 'magnetic inductance B in the literature') (Reichel, 1980). Magnetic flux is expressed as:

$$\Phi = B \cdot A \tag{4.8}$$

WAVELYNX EX. 1008, Pg. 19
WaveLynx Technologies v. ASSA Abloy, IPR2023-00730

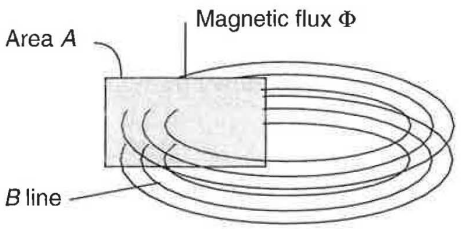


Figure 4.6 Relationship between magnetic flux Φ and flux density B

The material relationship between flux density B and field strength H (Figure 4.6) is expressed by the material equation:

$$B = \mu_0 \mu_r H = \mu H \tag{4.9}$$

The constant μ_0 is the magnetic field constant ($\mu_0 = 4\pi \times 10^{-6}$ Vs/Am) and describes the permeability (= magnetic conductivity) of a vacuum. The variable μ_r is called relative permeability and indicates how much greater than or less than μ_0 the permeability of a material is.

4.1.3 Inductance *L*

A magnetic field, and thus a magnetic flux Φ, will be generated around a conductor of any shape. This will be particularly intense if the conductor is in the form of a loop (coil). Normally, there is not one conduction loop, but N loops of the same area A, through which the same current I flows. Each of the conduction loops contributes the same proportion Φ to the total flux ψ (Paul, 1993).

$$\Psi = \sum_N \Phi_N = N \cdot \Phi = N \cdot \mu \cdot H \cdot A \tag{4.10}$$

The ratio of the interlinked flux ψ that arises in an area enclosed by current I, to the current in the conductor that encloses it (conductor loop) is denoted by *inductance* L (Figure 4.7):

$$L = \frac{\Psi}{I} = \frac{N \cdot \Phi}{I} = \frac{N \cdot \mu \cdot H \cdot A}{I} \tag{4.11}$$

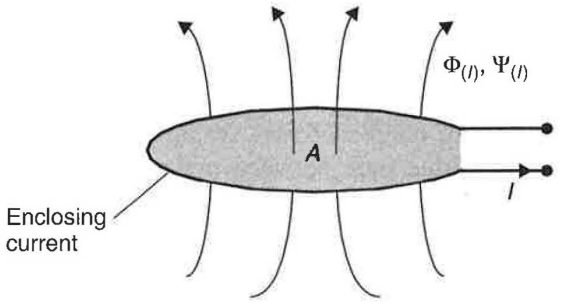


Figure 4.7 Definition of inductance L

WAVELYNX EX. 1008, Pg. 20
WaveLynx Technologies v. ASSA Abloy, IPR2023-00730

Inductance is one of the characteristic variables of conductor loops (coils). The inductance of a conductor loop (coil) depends totally upon the material properties (permeability) of the space that the flux flows through and the geometry of the layout.

4.1.3.1 Inductance of a conductor loop

If we assume that the diameter d of the wire used is very small compared to the diameter D of the conductor coil ($d/D < 0.0001$) a very simple approximation can be used:

$$L = N^2 \mu_0 R \cdot \ln\left(\frac{2R}{d}\right) \tag{4.12}$$

where R is the radius of the conductor loop and d is the diameter of the wire used.

4.1.4 Mutual inductance *M*

If a second conductor loop 2 (area A_2) is located in the vicinity of conductor loop 1 (area A_1), through which a current is flowing, then this will be subject to a proportion of the total magnetic flux Φ flowing through A_1. The two circuits are connected together by this partial flux or coupling flux. The magnitude of the coupling flux ψ_{21} depends upon the geometric dimensions of both conductor loops, the position of the conductor loops in relation to one another, and the magnetic properties of the medium (e.g. permeability) in the layout.

Similarly to the definition of the (self) inductance L of a conductor loop, the *mutual inductance* M_{21} of conductor loop 2 in relation to conductor loop 1 is defined as the ratio of the partial flux ψ_{21} enclosed by conductor loop 2, to the current I_1 in conductor loop 1 (Paul, 1993):

$$M_{21} = \frac{\Psi_{21}(I_1)}{I_1} = \oint_{A2} \frac{B_2(I_1)}{I_1} \cdot dA_2 \tag{4.13}$$

Similarly, there is also a mutual inductance M_{12}. Here, current I_2 flows through the conductor loop 2, thereby determining the coupling flux ψ_{12} in loop 1. The following relationship applies:

$$M = M_{12} = M_{21} \tag{4.14}$$

Mutual inductance describes the coupling of two circuits via the medium of a magnetic field (Figure 4.8). Mutual inductance is always present between two electric circuits. Its dimension and unit are the same as for inductance.

The coupling of two electric circuits via the magnetic field is the physical principle upon which inductively coupled RFID systems are based. Figure 4.9 shows a calculation of the mutual inductance between a transponder antenna and three different reader antennas, which differ only in diameter. The calculation is based upon the following values: M_1: $R = 55\,\text{cm}$, M_2: $R = 7.5\,\text{cm}$, M_3: $R = 1\,\text{cm}$, transponder: $R = 3.5\,\text{cm}$. $N = 1$ for all reader antennas.

The graph of *mutual inductance* shows a strong similarity to the graph of magnetic field strength H along the x axis. Assuming a homogeneous magnetic field, the mutual

WAVELYNX EX. 1008, Pg. 21
WaveLynx Technologies v. ASSA Abloy, IPR2023-00730

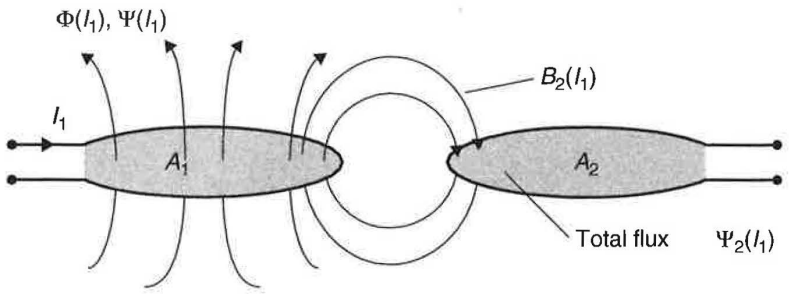


Figure 4.8 The definition of mutual inductance M_{21} by the coupling of two coils via a partial magnetic flow

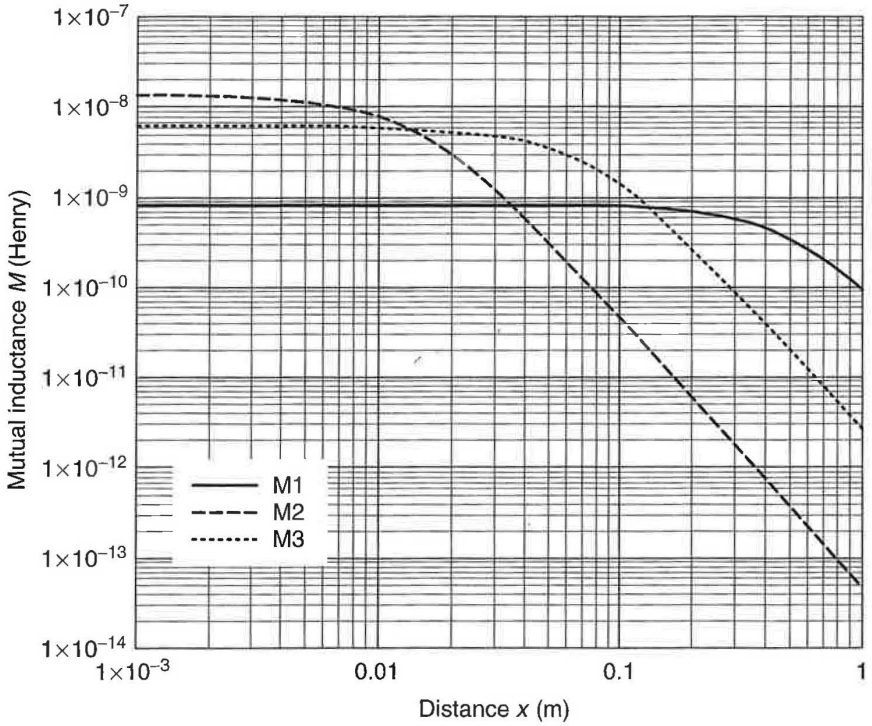


Figure 4.9 Graph of mutual inductance between reader and transponder antenna as the distance in the x direction increases

inductance M_{12} between two coils can be calculated using equation (4.13). It is found to be:

$$M_{12} = \frac{B_2(I_1) \cdot N_2 \cdot A_2}{I_1} = \frac{\mu_0 \cdot H(I_1) \cdot N_2 \cdot A_2}{I_1} \tag{4.15}$$

We first replace $H(I_1)$ with the expression in equation (4.4), and substitute $R^2\pi$ for A, thus obtaining:

$$M_{12} = \frac{\mu_0 \cdot N_1 \cdot R_1^2 \cdot N_2 \cdot R_2^2 \cdot \pi}{2\sqrt{(R_1^2 + x^2)^3}} \tag{4.16}$$

WAVELYNX EX. 1008, Pg. 22
WaveLynx Technologies v. ASSA Abloy, IPR2023-00730

In order to guarantee the homogeneity of the magnetic field in the area A_2 the condition $A_2 \leq A_1$ should be fulfilled. Furthermore, this equation only applies to the case where the x axes of the two coils lie on the same plane. Due to the relationship $M = M_{12} = M_{21}$ the mutual inductance can be calculated as follows for the case $A_2 \geq A_1$:

$$M_{21} = \frac{\mu_0 \cdot N_1 \cdot R_1^2 \cdot N_2 \cdot R_2^2 \cdot \pi}{2\sqrt{(R_2^2 + x^2)^3}} \tag{4.17}$$

4.1.5 Coupling coefficient *k*

Mutual inductance is a quantitative description of the flux coupling of two conductor loops. The *coupling coefficient* k is introduced so that we can make a qualitative prediction about the coupling of the conductor loops independent of their geometric dimensions. The following applies:

$$k = \frac{M}{\sqrt{L_1 \cdot L_2}} \tag{4.18}$$

The coupling coefficient always varies between the two extreme cases $0 \leq k \leq 1$.

- $k = 0$: Full decoupling due to great distance or magnetic shielding.
- $k = 1$: Total coupling. Both coils are subject to the same magnetic flux Φ. The transformer is a technical application of total coupling, whereby two or more coils are wound onto a highly permeable iron core.

An analytic calculation is only possible for very simple antenna configurations. For two parallel conductor loops centred on a single x axis the coupling coefficient according to Roz and Fuentes (n.d.) can be approximated from the following equation. However, this only applies if the radii of the conductor loops fulfil the condition $r_{\text{Transp}} \leq r_{\text{Reader}}$. The distance between the conductor loops on the x axis is denoted by x.

$$k(x) \approx \frac{r_{\text{Transp}}^2 \cdot r_{\text{Reader}}^2}{\sqrt{r_{\text{Transp}} \cdot r_{\text{Reader}}} \cdot \left(\sqrt{x^2 + r_{\text{Reader}}^2}\right)^3} \tag{4.19}$$

Due to the fixed link between the coupling coefficient and mutual inductance M, and because of the relationship $M = M_{12} = M_{21}$, the formula is also applicable to transmitter antennas that are smaller than the transponder antenna. Where $r_{\text{Transp}} \geq r_{\text{Reader}}$, we write:

$$k(x) \approx \frac{r_{\text{Transp}}^2 \cdot r_{\text{Reader}}^2}{\sqrt{r_{\text{Transp}} \cdot r_{\text{Reader}}} \cdot \left(\sqrt{x^2 + r_{\text{Transp}}^2}\right)^3} \tag{4.20}$$

The coupling coefficient $k(x) = 1$ (= 100%) is achieved where the distance between the conductor loops is zero ($x = 0$) and the antenna radii are identical ($r_{\text{Transp}} = r_{\text{Reader}}$),

WAVELYNX EX. 1008, Pg. 23
WaveLynx Technologies v. ASSA Abloy, IPR2023-00730

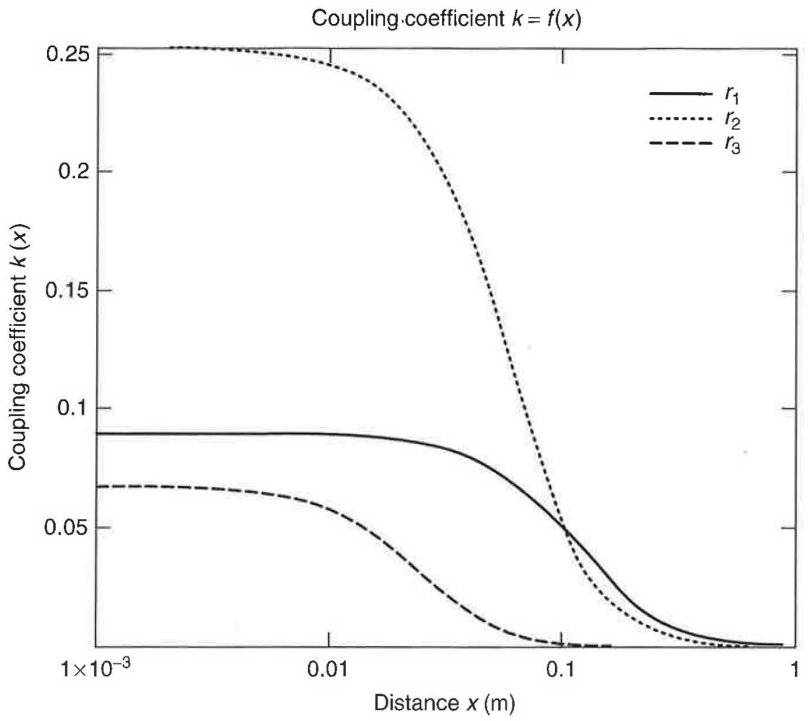


Figure 4.10 Graph of the coupling coefficient for different sized conductor loops. Transponder antenna: $r_{\text{Transp}} = 2\,\text{cm}$, reader antenna: $r_1 = 10\,\text{cm}$, $r_2 = 7.5\,\text{cm}$, $r_3 = 1\,\text{cm}$

because in this case the conductor loops are in the same place and are exposed to exactly the same magnetic flux ψ.

In practice, however, inductively coupled transponder systems operate with coupling coefficients that may be as low as 0.01 (<1%) (Figure 4.10).

4.1.6 Faraday's law

Any change to the magnetic flux Φ generates an electric field strength E_i. This characteristic of the magnetic field is described by *Faraday's law*.

The effect of the electric field generated in this manner depends upon the material properties of the surrounding area. Figure 4.11 shows some of the possible effects (Paul, 1993):

- Vacuum: in this case, the field strength E gives rise to an *electric rotational field*. Periodic changes in magnetic flux (high frequency current in an antenna coil) generate an electromagnetic field that propagates itself into the distance.
- Open conductor loop: an open circuit voltage builds up across the ends of an almost closed conductor loop, which is normally called *induced voltage*. This voltage corresponds with the line integral (path integral) of the field strength E that is generated along the path of the conductor loop in space.

WAVELYNX EX. 1008, Pg. 24
WaveLynx Technologies v. ASSA Abloy, IPR2023-00730

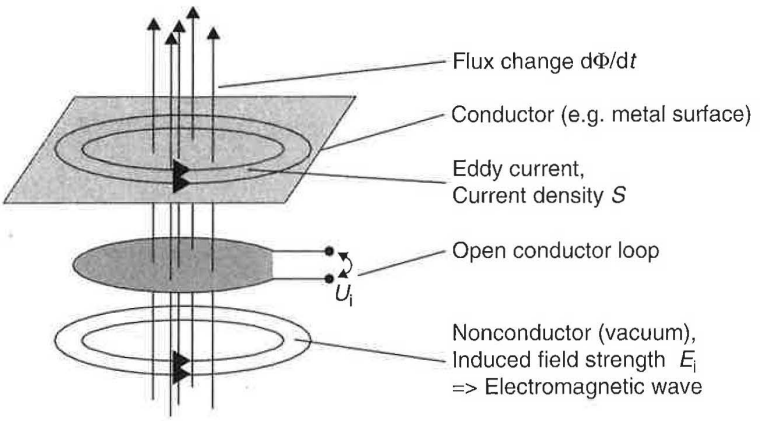


Figure 4.11 Induced electric field strength E in different materials. From top to bottom: metal surface, conductor loop and vacuum

- Metal surface: an electric field strength E is also induced in the metal surface. This causes free charge carriers to flow in the direction of the electric field strength. Currents flowing in circles are created, so-called *eddy currents*. This works against the exciting magnetic flux (Lenz's law), which may significantly damp the magnetic flux in the vicinity of *metal surfaces*. However, this effect is undesirable in inductively coupled RFID systems (installation of a transponder or reader antenna on a metal surface) and must therefore be prevented by suitable countermeasures (see Section 4.1.12.3).

In its general form Faraday's law is written as follows:

$$u_i = \oint E_i \cdot ds = -\frac{d\Psi(t)}{dt} \tag{4.21}$$

For a conductor loop configuration with N windings, we can also say that $u_i = N \cdot d\Psi/dt$. (The value of the contour integral $\int E_i \cdot ds$ can be increased N times if the closed integration path is carried out N times; Paul, 1993).

To improve our understanding of inductively coupled RFID systems we will now consider the effect of inductance on magnetically coupled conduction loops.

A time variant current $i_1(t)$ in conduction loop L_1 generates a time variant magnetic flux $d\Phi(i_1)/dt$. In accordance with the inductance law, a voltage is induced in the conductor loops L_1 and L_2 through which some degree of magnetic flux is flowing. We can differentiate between two cases:

- *Self-inductance*: the flux change generated by the current change di_n/dt induces a voltage u_n in the same conductor circuit.
- *Mutual inductance*: the flux change generated by the current change di_n/dt induces a voltage in the adjacent conductor circuit L_m. Both circuits are coupled by mutual inductance.

Figure 4.12 shows the equivalent circuit diagram for coupled conductor loops. In an inductively coupled RFID system L_1 would be the transmitter antenna of the reader.

WAVELYNX EX. 1008, Pg. 25
WaveLynx Technologies v. ASSA Abloy, IPR2023-00730

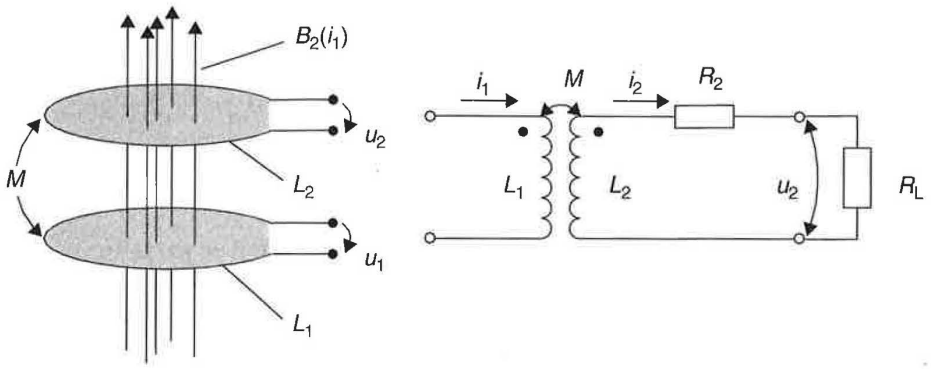


Figure 4.12 Left, magnetically coupled conductor loops; right, equivalent circuit diagram for magnetically coupled conductor loops

L_2 represents the antenna of the transponder, where R_2 is the *coil resistance* of the transponder antenna. The current consumption of the data memory is symbolised by the load resistor R_L.

A time varying flux in the conductor loop L_1 induces voltage u_{2i} in the conductor loop L_2 due to mutual inductance M. The flow of current creates an additional voltage drop across the coil resistance R_2, meaning that the voltage u_2 can be measured at the terminals. The current through the load resistor R_L is calculated from the expression u_2/R_L. The current through L_2 also generates an additional magnetic flux, which opposes the magnetic flux $\Psi_1(i_1)$. The above is summed up in the following equation:

$$u_2 = +\frac{d\Psi_2}{dt} = M\frac{di_1}{dt} - L_2\frac{di_2}{dt} - i_2R_2 \tag{4.22}$$

Because, in practice, i_1 and i_2 are sinusoidal (HF) alternating currents, we write equation (4.22) in the more appropriate complex notation (where $\omega = 2\pi f$):

$$u_2 = j\omega M \cdot i_1 - j\omega L_2 \cdot i_2 - i_2R_2 \tag{4.23}$$

If i_2 is replaced by u_2/R_L in equation (4.23), then we can solve the equation for u_2:

$$u_2 = \frac{j\omega M \cdot i_1}{1 + \dfrac{j\omega L_2 + R_2}{R_L}} \quad \begin{cases} \rightarrow R_L \rightarrow \infty: u_2 = j\omega M \cdot i_1 \\ \rightarrow R_L \rightarrow 0: u_2 \rightarrow 0 \end{cases} \tag{4.24}$$

4.1.7 Resonance

The voltage u_2 induced in the transponder coil is used to provide the power supply to the data memory (*microchip*) of a passive transponder (see Section 4.1.8.1). In order to significantly improve the efficiency of the equivalent circuit illustrated in Figure 4.12, an additional capacitor C_2 is connected in parallel with the transponder coil L_2 to form a *parallel resonant circuit* with a *resonant frequency* that corresponds with the

WAVELYNX EX. 1008, Pg. 26
WaveLynx Technologies v. ASSA Abloy, IPR2023-00730

operating frequency of the RFID system in question.[1] The resonant frequency of the parallel resonant circuit can be calculated using the Thomson equation:

$$f = \frac{1}{2\pi\sqrt{L_2 \cdot C_2}} \tag{4.25}$$

In practice, C_2 is made up of a parallel capacitor C_2' and a parasitic capacitance C_p from the real circuit. $C_2 = (C_2' + C_p)$. The required capacitance for the parallel capacitor C_2' is found using the Thomson equation, taking into account the parasitic capacitance C_p:

$$C_2' = \frac{1}{(2\pi f)^2 L_2} - C_p \tag{4.26}$$

Figure 4.13 shows the equivalent circuit diagram of a real transponder. R_2 is the natural resistance of the transponder coil L_2 and the current consumption of the data carrier (chip) is represented by the load resistor R_L.

If a voltage $u_{Q2} = u_i$ is induced in the coil L_2, the following voltage u_2 can be measured at the data carrier load resistor R_L in the equivalent circuit diagram shown in Figure 4.13:

$$u_2 = \frac{u_{Q2}}{1 + (j\omega L_2 + R_2) \cdot \left(\frac{1}{R_L} + j\omega C_2\right)} \tag{4.27}$$

We now replace the induced voltage $u_{Q2} = u_i$ by the factor responsible for its generation, $u_{Q2} = u_i = j\omega M \cdot i_1 = \omega \cdot k \cdot \sqrt{L_1 \cdot L_2} \cdot i_1$, thus obtaining the relationship

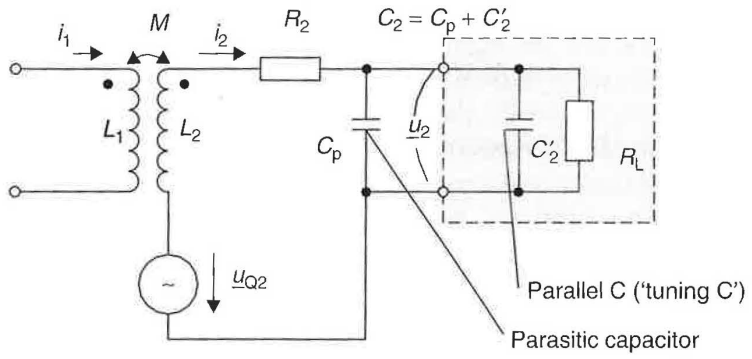


Figure 4.13 Equivalent circuit diagram for magnetically coupled conductor loops. Transponder coil L_2 and parallel capacitor C_2 form a parallel resonant circuit to improve the efficiency of voltage transfer. The transponder's data carrier is represented by the grey box

[1] However, in 13.56 MHz systems with anticollision procedures, the resonant frequency selected for the transponder is often 1–5 MHz higher to minimise the effect of the interaction between transponders on overall performance. This is because the overall resonant frequency of two transponders directly adjacent to one another is always lower than the resonant frequency of a single transponder.

WAVELYNX EX. 1008, Pg. 27
WaveLynx Technologies v. ASSA Abloy, IPR2023-00730

between voltage u_2 and the magnetic coupling of transmitter coil and transponder coil:

$$u_2 = \frac{j\omega M \cdot i_1}{1 + (j\omega L_2 + R_2) \cdot \left(\frac{1}{R_L} + j\omega C_2\right)} \tag{4.28}$$

and:

$$u_2 = \frac{j\omega \cdot k \cdot \sqrt{L_1 \cdot L_2} \cdot i_1}{1 + (j\omega L_2 + R_2) \cdot \left(\frac{1}{R_L} + j\omega C_2\right)} \tag{4.29}$$

or in the non-complex form (Jurisch, 1994):

$$u_2 = \frac{\omega \cdot k \cdot \sqrt{L_1 L_2} \cdot i_1}{\sqrt{\left(\frac{\omega L_2}{R_L} + \omega R_2 C_2\right)^2 + \left(1 - \omega^2 L_2 C_2 + \frac{R_2}{R_L}\right)^2}} \tag{4.30}$$

where $C_2 = C_2' + C_p$.

Figure 4.14 shows the simulated graph of u_2 with and without resonance over a large frequency range for a possible transponder system. The current i_1 in the transmitter antenna (and thus also $\Phi(i_1)$), inductance L_2, mutual inductance M, R_2 and R_L are held constant over the entire frequency range.

We see that the graph of voltage u_2 for the circuit with the coil alone (circuit from Figure 4.12) is almost identical to that of the *parallel resonant circuit* (circuit from

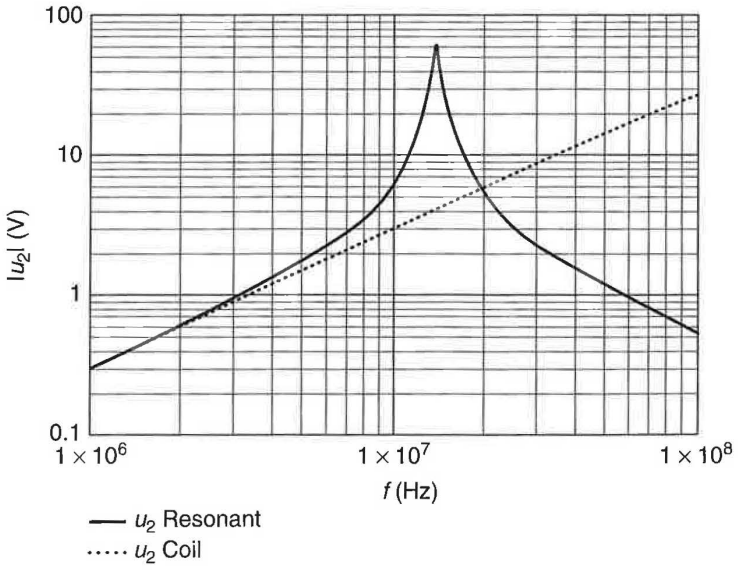


Figure 4.14 Plot of voltage at a transponder coil in the frequency range 1 to 100 MHz, given a constant magnetic field strength H or constant current i_1. A transponder coil with a parallel capacitor shows a clear voltage step-up when excited at its resonant frequency ($f_{RES} = 13.56$ MHz)

WAVELYNX EX. 1008, Pg. 28
WaveLynx Technologies v. ASSA Abloy, IPR2023-00730

Figure 4.13) at frequencies well below the resonant frequencies of both circuits, but that when the resonant frequency is reached, voltage u_2 increases by more than a power of ten in the parallel resonant circuit compared to the voltage u_2 for the coil alone. Above the resonant frequency, however, voltage u_2 falls rapidly in the parallel resonant circuit, even falling below the value for the coil alone.

For transponders in the frequency range below 135 kHz, the transponder coil L_2 is generally connected in parallel with a chip capacitor ($C_2' = 20-220$ pF) to achieve the desired resonant frequency. At the higher frequencies of 13.56 MHz and 27.125 MHz, the required capacitance C_2 is usually so low that it is provided by the input capacitance of the data carrier together with the parasitic capacitance of the transponder coil.

Let us now investigate the influence of the circuit elements R_2, R_L and L_2 on voltage u_2. To gain a better understanding of the interactions between the individual parameters we will now introduce the Q factor (the Q factor crops up again when we investigate the connection of transmitter antennas in Section 11.4.1.3). We will refrain from deriving formulas because the electric resonant circuit is dealt with in detail in the background reading.

The *Q factor* is a measure of the voltage and current step-up in the resonant circuit at its resonant frequency. Its reciprocal 1/Q denotes the expressively named *circuit damping* d. The Q factor is very simple to calculate for the equivalent circuit in Figure 4.13. In this case ω is the angular frequency ($\omega = 2\pi f$) of the transponder resonant circuit:

$$Q = \frac{1}{R_2 \cdot \sqrt{\frac{C_2}{L_2}} + \frac{1}{R_L} \cdot \sqrt{\frac{L_2}{C_2}}} = \frac{1}{\frac{R_2}{\omega L_2} + \frac{\omega L_2}{R_L}} \tag{4.31}$$

A glance at equation (4.31) shows that when $R_2 \to \infty$ and $R_L \to 0$, the Q factor also tends towards zero. On the other hand, when the transponder coil has a very low coil resistance $R_2 \to 0$ and there is a high load resistor $R_L \gg 0$ (corresponding with very low transponder chip power consumption), very high Q factors can be achieved. The voltage u_2 is now proportional to the quality of the resonant circuit, which means that the dependency of voltage u_2 upon R_2 and R_L is clearly defined.

Voltage u_2 thus tends towards zero where $R_2 \to \infty$ and $R_L \to 0$. At a very low transponder coil resistance $R_2 \to 0$ and a high value load resistor $R_L \gg 0$, on the other hand, a very high voltage u_2 can be achieved (compare equation (4.30)).

It is interesting to note the path taken by the graph of voltage u_2 when the inductance of the transponder coil L_2 is changed, thus maintaining the resonance condition (i.e. $C_2 = 1/\omega^2 L_2$ for all values of L_2). We see that for certain values of L_2, voltage u_2 reaches a clear peak (Figure 4.15).

If we now consider the graph of the Q factor as a function of L_2 (Figure 4.16), then we observe a maximum at the same value of transponder inductance L_2. The maximum voltage $u_2 = f(L_2)$ is therefore derived from the maximum Q factor, $Q = f(L_2)$, at this point.

This indicates that for every pair of parameters (R_2, R_L), there is an inductance value L_2 at which the Q factor, and thus also the supply voltage u_2 to the data carrier, is at a maximum. This should always be taken into consideration when designing a transponder, because this effect can be exploited to optimise the energy range of

WAVELYNX EX. 1008, Pg. 29
WaveLynx Technologies v. ASSA Abloy, IPR2023-00730

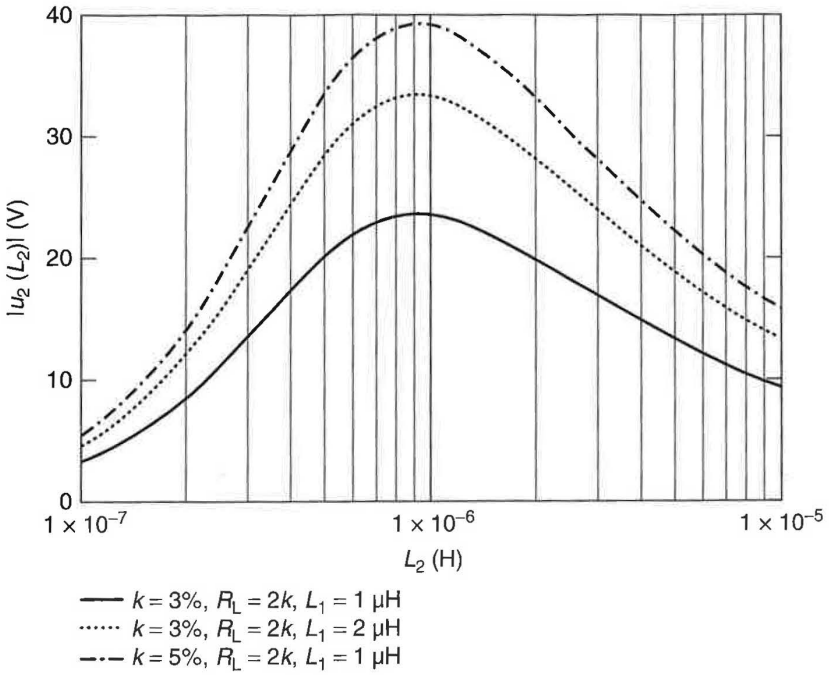


Figure 4.15 Plot of voltage u_2 for different values of transponder inductance L_2. The resonant frequency of the transponder is equal to the transmission frequency of the reader for all values of L_2 ($i_1 = 0.5\,\text{A}$, $f = 13.56\,\text{MHz}$, $R_2 = 1\,\Omega$)

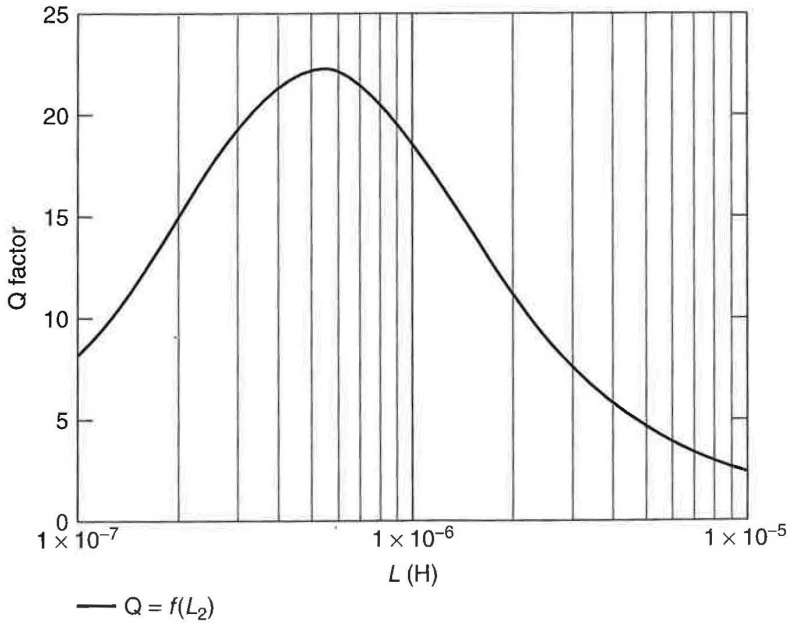


Figure 4.16 Graph of the Q factor as a function of transponder inductance L_2, where the resonant frequency of the transponder is constant ($f = 13.56\,\text{MHz}$, $R_2 = 1\,\Omega$)

WAVELYNX EX. 1008, Pg. 30
WaveLynx Technologies v. ASSA Abloy, IPR2023-00730

an inductively coupled RFID system. However, we must also bear in mind that the influence of component tolerances in the system also reaches a maximum in the Q_{max} range. This is particularly important in systems designed for mass production. Such systems should be designed so that reliable operation is still possible in the range $Q \ll Q_{max}$ at the maximum distance between transponder and reader.

R_L should be set at the same value as the input resistance of the data carrier after setting the 'power on' reset, i.e. before the activation of the voltage regulator, as is the case for the maximum energy range of the system.

4.1.8 Practical operation of the transponder

4.1.8.1 Power supply to the transponder

Transponders are classified as active or passive depending upon the type of power supply they use.

Active transponders incorporate their own battery to provide the power supply to the data carrier. In these transponders, the voltage u_2 is generally only required to generate a 'wake up' signal. As soon as the voltage u_2 exceeds a certain limit this signal is activated and puts the data carrier into operating mode. The transponder returns to the power saving 'sleep' or 'stand-by mode' after the completion of a transaction with the reader, or when the voltage u_2 falls below a minimum value.

In *passive transponders* the data carrier has to obtain its power supply from the voltage u_2. To achieve this, the voltage u_2 is converted into direct current using a low loss bridge rectifier and then smoothed. A simple basic circuit for this application is shown in Figure 3.18.

4.1.8.2 Voltage regulation

The induced voltage u_2 in the transponder coil very rapidly reaches high values due to resonance step-up in the resonant circuit. Considering the example in Figure 4.14, if we increase the coupling coefficient k — possibly by reducing the gap between reader and transponder — or the value of the load resistor R_L, then voltage u_2 will reach a level much greater than 100 V. However, the operation of a data carrier requires a constant *operating voltage* of 3–5 V (after rectification).

In order to regulate voltage u_2 independently of the coupling coefficient k or other parameters, and to hold it constant in practice, a voltage-dependent shunt resistor R_S is connected in parallel with the load resistor R_L. The equivalent circuit diagram for this is shown in Figure 4.17.

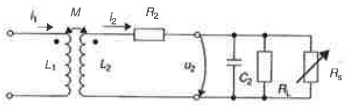


Figure 4.17 Operating principle for voltage regulation in the transponder using a shunt regulator

As induced voltage $u_{Q2} = u_i$ increases, the value of the shunt resistor R_S falls, thus reducing the quality of the transponder resonant circuit to such a degree that the voltage u_2 remains constant. To calculate the value of the shunt resistor for different variables, we refer back to equation (4.29) and introduce the parallel connection of R_L and R_S in place of the constant load resistor R_L. The equation can now be solved with respect to R_S. The variable voltage u_2 is replaced by the constant voltage u_{Transp} — the desired input voltage of the data carrier — giving the following equation for R_S:

$$R_S = \left| \frac{1}{\left(\frac{j\omega \cdot k \cdot \sqrt{L_1 L_2} \cdot i_1}{u_{Transp}} \right) - 1} - j\omega C_2 - \frac{1}{R_L} \right| \quad | u_{2\text{-unreg}} > u_{Transp} \qquad (4.32)$$

Figure 4.18 shows the graph of voltage u_2 when such an 'ideal' shunt regulator is used. Voltage u_2 initially increases in proportion with the coupling coefficient k. When u_2 reaches its desired value, the value of the shunt resistor begins to fall in inverse proportion to k, thus maintaining an almost constant value for voltage u_2.

Figure 4.19 shows the variable value of the shunt resistor R_S as a function of the coupling coefficient. In this example the value range for the shunt resistor covers several powers of ten. This can only be achieved using a semiconductor circuit, therefore so-called *shunt* or *parallel regulators* are used in inductively coupled transponders. These terms describe an electronic regulator circuit, the internal resistance of which

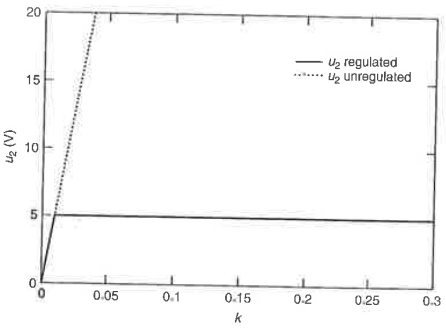


Figure 4.18 Example of the path of voltage u_2 with and without shunt regulation in the transponder, where the coupling coefficient k is varied by altering the distance between transponder and reader antenna. (The calculation is based upon the following parameters: $i_1 = 0.5$ A, $L_1 = 1\,\mu$H, $L_2 = 3.5\,\mu$H, $R_L = 2\,k\Omega$, $C_2 = 1/\omega_2 L_2$)

WAVELYNX EX. 1008, Pg. 31
WaveLynx Technologies v. ASSA Abloy, IPR2023-00730

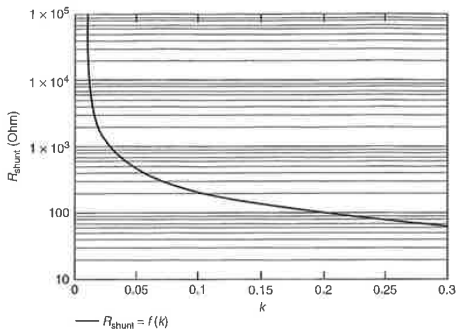


Figure 4.19 The value of the shunt resistor R_S must be adjustable over a wide range to keep voltage u_2 constant regardless of the coupling coefficient k (parameters as Figure 4.18)

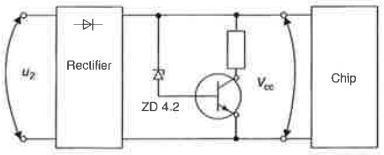


Figure 4.20 Example circuit for a simple shunt regulator

falls disproportionately sharply when a threshold voltage is exceeded. A simple shunt regulator based upon a zener diode (Nührmann, 1994) is shown in Figure 4.20.

4.1.9 Interrogation field strength H_{min}

We can now use the results obtained in Section 4.1.7 to calculate the *interrogation field strength* of a transponder. This is the minimum field strength H_{min} (at a maximum distance x between transponder and reader) at which the supply voltage u_2 is just high enough for the operation of the data carrier.

However, u_2 is not the internal operating voltage of the data carrier (3V or 5V) here; it is the *HF input voltage* at the terminal of the transponder coil L_2 on the data carrier, i.e. prior to rectification. The voltage regulator (shunt regulator) should not yet be active at this supply voltage. R_L corresponds with the input resistance of the data carrier after the 'power on reset', C_2 is made up of the input capacitance

C_p of the data carrier (chip) and the parasitic capacitance of the transponder layout $C_2' : C_2 = (C_2' + C_p)$.

The inductive voltage (source voltage $u_{Q2} = u_i$) of a transponder coil can be calculated using equation (4.21) for the general case. If we assume a homogeneous, sinusoidal magnetic field in air (permeability constant = μ_0) we can derive the following, more appropriate, formula:

$$u_i = \mu_0 \cdot A \cdot N \cdot \omega \cdot H_{eff} \tag{4.33}$$

where H_{eff} is the effective field strength of a sinusoidal magnetic field, ω is the angular frequency of the magnetic field, N is the number of windings of the transponder coil L_2, and A is the cross-sectional area of the transponder coil.

We now replace $u_{Q2} = u_i = j\omega M \cdot i_1$ from equation (4.29) with equation (4.33) and thus obtain the following equation for the circuit in Figure 4.13:

$$u_2 = \frac{j\omega \cdot \mu_0 \cdot H_{eff} \cdot A \cdot N}{1 + (j\omega L_2 + R_2)\left(\frac{1}{R_L} + j\omega C_2\right)} \tag{4.34}$$

Multiplying out the denominator:

$$u_2 = \frac{j\omega \cdot \mu_0 \cdot H_{eff} \cdot A \cdot N}{j\omega\left(\frac{L_2}{R_L} + R_2 C_2\right) + \left(1 - \omega^2 L_2 C_2 + \frac{R_2}{R_L}\right)} \tag{4.35}$$

We now solve this equation for H_{eff} and obtain the value of the complex form. This yields the following relationship for the interrogation field H_{min} in the general case:

$$H_{min} = \frac{u_2 \cdot \sqrt{\left(\frac{\omega L_2}{R_L} + \omega R_2 C_2\right)^2 + \left(1 - \omega^2 L_2 C_2 + \frac{R_2}{R_L}\right)^2}}{\omega \cdot \mu_0 \cdot A \cdot N} \tag{4.36}$$

A more detailed analysis of equation (4.36) shows that the interrogation field strength is dependent upon the frequency $\omega = 2\pi f$ in addition to the antenna area A, the number of windings N (of the transponder coil), the minimum voltage u_2 and the input resistance R_2. This is not surprising, because we have determined a resonance step-up of u_2 at the resonant frequency of the transponder resonant circuit. Therefore, when the transmission frequency of the reader corresponds with the resonant frequency of the transponder, the interrogation field strength H_{min} is at its minimum value.

To optimise the interrogation sensitivity of an inductively coupled RFID system, the resonant frequency of the transponder should be matched precisely to the transmission frequency of the reader. Unfortunately, this is not always possible in practice. First, tolerances occur during the manufacture of a transponder, which lead to a deviation in the transponder resonant frequency. Second, there are also technical reasons for setting the resonant frequency of the transponder a few percentage points higher than the transmission frequency of the reader (for example in systems using anticollision procedures to keep the interaction of nearby transponders low).

WAVELYNX EX. 1008, Pg. 32
WaveLynx Technologies v. ASSA Abloy, IPR2023-00730

Some semiconductor manufacturers incorporate additional smoothing capacitors into the transponder chip to smooth out frequency deviations in the transponder caused by manufacturing tolerances (see Figure 3.28, 'tuning C'). During manufacture the transponder is adjusted to the desired frequency by switching individual smoothing capacitors on and off (Schürmann, 1993).

In equation (4.36) the resonant frequency of the transponder is expressed as the product L_2C_2. This is not recognisable at first glance. In order to make a direct prediction regarding the frequency dependency of interrogation sensitivity, we rearrange equation (4.25) to obtain:

$$L_2C_2 = \frac{1}{(2\pi f_0)^2} = \frac{1}{\omega_0^2} \tag{4.37}$$

By substituting this expression into the right-hand term under the root of equation (4.36) we obtain a function in which the dependence of the interrogation field strength H_{min} on the relationship between the transmission frequency of the reader (ω) and the resonant frequency of the transponder (ω_0) is clearly expressed. This is based upon the assumption that the change in the resonant frequency of the transponder is caused by a change in the capacitance of C_2 (e.g. due to temperature dependence or manufacturing tolerances of this capacitance), whereas the inductance L_2 of the coil remains constant. To express this, the capacitor C_2 in the left-hand term under the root of equation (4.36) is replaced by $C_2 = (\omega_0^2 \cdot L_2)^{-1}$:

$$H_{min} = \frac{u_2 \cdot \sqrt{\omega^2 \left(\frac{L_2}{R_L} + \frac{R_2}{\omega_0^2 L_2}\right)^2 + \left(\frac{\omega_0^2 - \omega^2}{\omega_0^2} + \frac{R_2}{R_L}\right)^2}}{\omega \mu_0 \cdot A \cdot N} \tag{4.38}$$

Therefore a deviation of the transponder resonant frequency from the transmission frequency of the reader will lead to a higher transponder interrogation field strength and thus to a lower *read range* (Figure 4.21).

4.1.9.1 Energy range of transponder systems

If the interrogation field strength of a transponder is known, then we can also assess the energy range associated with a certain reader. The *energy range* of a transponder is the distance from the reader antenna at which there is just enough energy to operate the transponder (defined by $u_{2\,min}$ and R_L). However, the question of whether the energy range obtained corresponds with the maximum functional range of the system also depends upon whether the data transmitted from the transponder can be detected by the reader at the distance in question.

Given a known antenna current[2] I, radius R, and number of windings of the transmitter antenna N_1, the path of the field strength in the x direction can be calculated using equation (4.3) (see Section 4.1.1.1). If we solve the equation with respect to x

[2] If the antenna current of the transmitter antenna is not known it can be calculated from the measured field strength $H(x)$ at a distance x, where the antenna radius R and the number of windings N_1 are known (see Section 4.1.1.1).

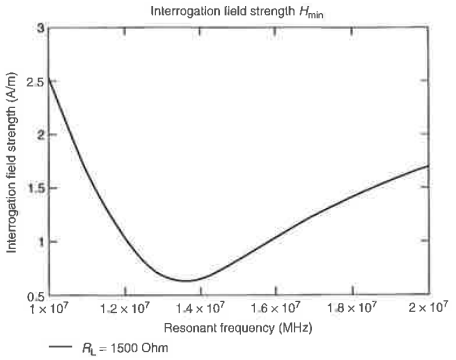


Figure 4.21 Interrogation sensitivity of a contactless smart card where the transponder resonant frequency is detuned in the range 10–20 MHz ($N = 4$, $A = 0.05 \times 0.08\,m^2$, $u_2 = 5V$, $L_2 = 3.5\,\mu H$, $R_2 = 5\,\Omega$, $R_L = 1.5\,k\Omega$). If the transponder resonant frequency deviates from the transmission frequency (13.56 MHz) of the reader an increasingly high field strength is required to address the transponder. In practical operation this results in a reduction of the read range

we obtain the following relationship between the energy range and interrogation field H_{min} of a transponder for a given reader:

$$x = \sqrt{\sqrt{\left(\frac{I \cdot N_1 \cdot R^2}{2 \cdot H_{min}}\right)^2} - R^2} \tag{4.39}$$

As an example (see Figure 4.22), let us now consider the energy range of a transponder as a function of the power consumption of the data carrier ($R_L = u_2/i_2$). The reader in this example generates a field strength of 0.115 A/m at a distance of 80 cm from the transmitter antenna (radius R of transmitter antenna: 40 cm). This is a typical value for RFID systems in accordance with ISO 15693.

As the current consumption of the transponder (lower R_L) increases, the interrogation sensitivity of the transponder also increases and the energy range falls.

The maximum energy range of the transponder is determined by the distance between transponder and reader antenna at which the minimum power supply $u_{2\,min}$ required for the operation of the data carrier exists even with an unloaded transponder resonant circuit (i.e. $i_2 \to 0$, $R_L \to \infty$). Where distance $x = 0$ the maximum current i_2 represents a limit, above which the supply voltage for the data carrier falls below $u_{2\,min}$, which means that the reliable operation of the data carrier can no longer be guaranteed in this operating state.

WAVELYNX EX. 1008, Pg. 33
WaveLynx Technologies v. ASSA Abloy, IPR2023-00730

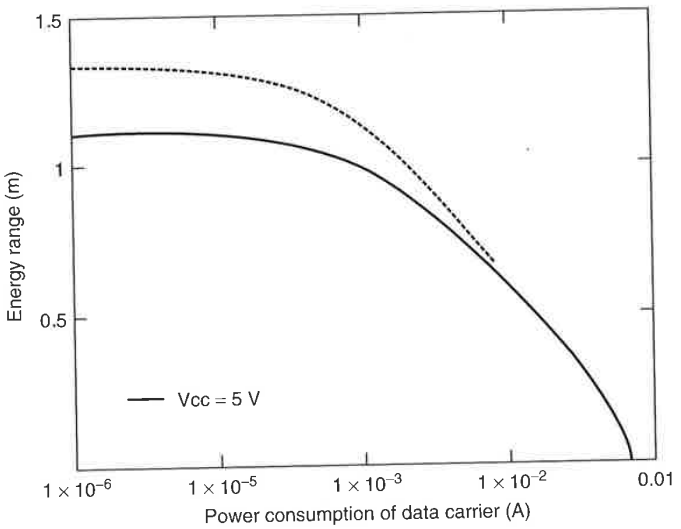


Figure 4.22 The energy range of a transponder also depends upon the power consumption of the data carrier (R_L). The transmitter antenna of the simulated system generates a field strength of 0.115 A/m at a distance of 80 cm, a value typical for RFID systems in accordance with ISO 15693 (transmitter: $I = 1$A, $N_1 = 1$, $R = 0.4$ m. Transponder: $A = 0.048 \times 0.076\,m^2$ (smart card), $N = 4$, $L_2 = 3.6\,\mu H$, $u_{2\,min} = 5V/3V$)

4.1.9.2 Interrogation zone of readers

In the calculations above the implicit assumption was made of a homogeneous magnetic field H parallel to the coil axis x. A glance at Figure 4.23 shows that this only applies for an arrangement of reader coil and transponder coil with a common central axis x. If the transponder is tilted away from this central axis or displaced in the direction of the y or z axis this condition is no longer fulfilled.

If a coil is magnetised by a magnetic field H, which is tilted by the angle ϑ in relation to the central axis of the coil, then in very general terms the following applies:

$$u_{0\vartheta} = u_0 \cdot \cos(\vartheta) \tag{4.40}$$

where u_0 is the voltage that is induced when the coil is perpendicular to the magnetic field. At an angle $\vartheta = 90°$, in which case the field lines run in the plane of the coil radius R, no voltage is induced in the coil.

As a result of the bending of the *magnetic field lines* in the entire area around the reader coil, here too there are different angles ϑ of the magnetic field H in relation to the transponder coil. This leads to a characteristic *interrogation zone* (Figure 4.24, grey area) around the reader antenna. Areas with an angle $\vartheta = 0°$ in relation to the transponder antenna — for example along the coil axis x, but also to the side of the antenna windings (returning field lines) — give rise to an optimal read range. Areas in which the magnetic field lines run parallel to the plane of the transponder coil radius

WAVELYNX EX. 1008, Pg. 34
WaveLynx Technologies v. ASSA Abloy, IPR2023-00730

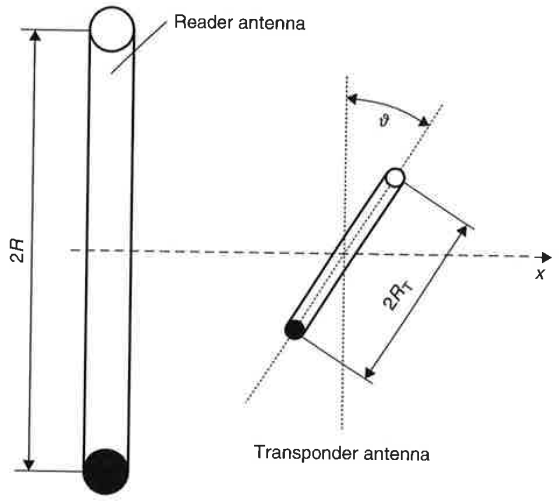


Figure 4.23 Cross-section through reader and transponder antennas. The transponder antenna is tilted at an angle ϑ in relation to the reader antenna

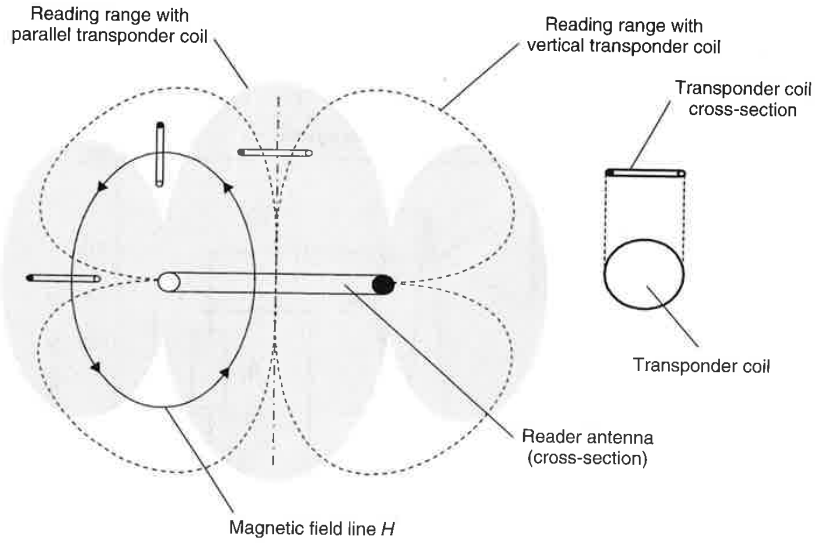


Figure 4.24 Interrogation zone of a reader at different alignments of the transponder coil

R — for example, exactly above and below the coil windings — exhibit a significantly reduced read range. If the transponder itself is tilted through 90° a completely different picture of the interrogation zone emerges (Figure 4.24, dotted line). Field lines that run parallel to the R-plane of the reader coil now penetrate the transponder coil at an angle $\vartheta = 0°$ and thus lead to an optimal *range* in this area.

WAVELYNX EX. 1008, Pg. 35
WaveLynx Technologies v. ASSA Abloy, IPR2023-00730

signal from the transponder that arrives at the reader, then, all other things being equal, the transmission power must be multiplied by sixteen! THIS IS NOT CORRECT. I THINK HE MEANT TO SAY IF THE DISTANCE IS DOUBLED TO GET THE SAME REFLECTED POWER WE NEED TO 16X THE TRANSMIT POWER.

4.2.5 Antennas

The creation of electromagnetic waves has already been described in detail in the previous section (see also Sections 4.1.6 and 4.2.1). The laws of physics tell us that the radiation of electromagnetic waves can be observed in all conductors that carry voltage and/or current. In contrast to these effects, which tend to be parasitic, an *antenna* is a component in which the radiation or reception of electromagnetic waves has been to a large degree optimised for certain frequency ranges by the fine-tuning of design properties. In this connection, the behaviour of an antenna can be precisely predicted and is exactly defined mathematically.

4.2.5.1 Gain and directional effect

Section 4.2.2 demonstrated how the power P_{EIRP} emitted from an *isotropic emitter* at a distance r is distributed in a fully uniform manner over a spherical surface area. If we integrate the power density S of the electromagnetic wave over the entire surface area of the sphere the result we obtain is, once again, the power P_{EIRP} emitted by the isotropic emitter.

$$P_{\mathrm{EIRP}} = \int_{A_{\mathrm{sphere}}} S \cdot \mathrm{d}A \tag{4.68}$$

However, a real antenna, for example a dipole, does not radiate the supplied power uniformly in all directions. For example, no power at all is radiated by a *dipole antenna* in the axial direction in relation to the antenna.

Equation (4.68) applies for all types of antennas. If the antenna emits the supplied power with varying intensity in different directions, then equation (4.68) can only be fulfilled if the radiation density S is greater in the preferred direction of the antenna than would be the case for an isotropic emitter. Figure 4.62 shows the *radiation pattern* of a dipole antenna in comparison to that of an isotropic emitter. The length of the vector $G(\Theta)$ indicates the relative radiation density in the direction of the vector. In the *main radiation direction* (G_{i}) the radiation density can be calculated as follows:

$$S = \frac{P_{\mathrm{I}} \cdot G_{\mathrm{i}}}{4\pi \cdot r^2} \tag{4.69}$$

P_{I} is the power supplied to the antenna. G_{i} is termed the gain of the antenna and indicates the factor by which the radiation density S is greater than that of an isotropic emitter at the same transmission power.

An important radio technology term in this connection is the *EIRP* (effective isotropic radiated power).

$$P_{\mathrm{EIRP}} = P_{\mathrm{I}} \cdot G_{\mathrm{i}} \tag{4.70}$$

This figure can often be found in radio licensing regulations (e.g. Section 5.2.4) and indicates the transmission power at which an isotropic emitter (i.e. $G_{\mathrm{i}} = 1$) would

WAVELYNX EX. 1008, Pg. 36
WaveLynx Technologies v. ASSA Abloy, IPR2023-00730

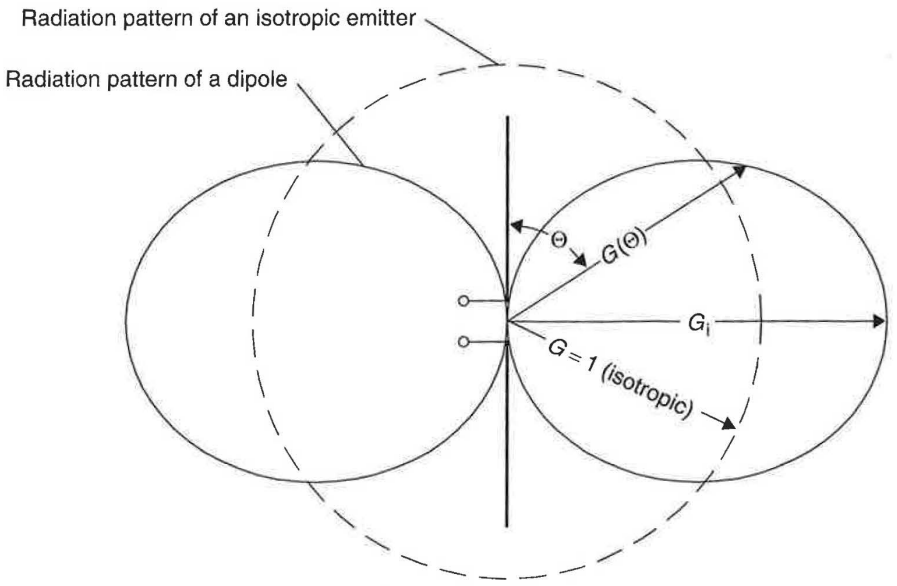


Figure 4.62 Radiation pattern of a dipole antenna in comparison to the radiation pattern of an isotropic emitter

have to be supplied in order to generate a defined radiation power at distance r. An antenna with a gain G_i may therefore only be supplied with a transmission power P_1 that is lower by this factor so that the specified limit value is not exceeded:

$$P_1 = \frac{P_{EIRP}}{G_i} \tag{4.71}$$

4.2.5.2 EIRP and ERP

In addition to power figures in EIRP we frequently come across the power figure ERP (equivalent radiated power) in radio regulations and technical literature. The ERP is also a reference power figure. However, in contrast to the EIRP, ERP relates to a dipole antenna rather than a spherical emitter. An ERP power figure thus expresses the transmission power at which a dipole antenna must be supplied in order to generate a defined emitted power at a distance of r. Since the gain of the dipole antenna

Table 4.7 In order to emit a constant EIRP in the main radiation direction less transmission power must be supplied to the antenna as the antenna gain G increases

EIRP = 4 W	**Power P_1 fed to the antenna**
Isotropic emitter $G_i = 1$	4 W
Dipole antenna	2.44 W
Antenna $G_i = 3$	1.33 W

WAVELYNX EX. 1008, Pg. 37
WaveLynx Technologies v. ASSA Abloy, IPR2023-00730

($G_i = 1.64$) in relation to an isotropic emitter is known, it is easy to convert between the two figures:

$$P_{EIRP} = P_{ERP} \cdot 1.64 \tag{4.72}$$

4.2.5.3 Input impedance

A particularly important property of the antenna is the complex *input impedance* Z_A. This is made up of a complex resistance X_A, a loss resistance R_V and the so-called *radiation resistance* R_r:

$$Z_A = R_r + R_V + jX_A \tag{4.73}$$

The loss resistance R_V is an effective resistance and describes all losses resulting from the ohmic resistance of all current-carrying line sections of the antenna (Figure 4.63). The power converted by this resistance is converted into heat.

The radiation resistance R_r also takes the units of an effective resistance but the power converted within it corresponds with the power emitted from the antenna into space in the form of electromagnetic waves.

At the operating frequency (i.e. the resonant frequency of the antenna) the complex resistance X_A of the antenna tends towards zero. For a loss-free antenna (i.e. $R_V = 0$):

$$Z_A(f_{RES}) = R_r \tag{4.74}$$

The input impedance of an ideal antenna in the resonant case is thus a real resistance with the value of the radiation resistance R_r. For a $\lambda/2$ dipole the radiation resistance $R_r = 73\ \Omega$.

4.2.5.4 Effective aperture and scatter aperture

The maximum received power that can be drawn from an antenna, given optimal alignment and correct polarisation, is proportional to the power density S of an incoming

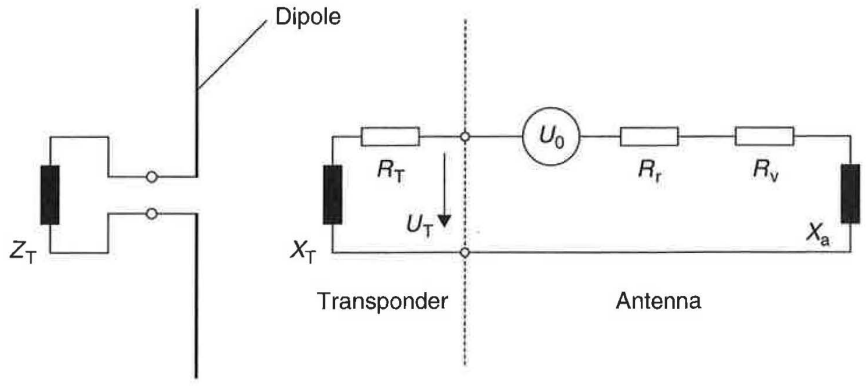


Figure 4.63 Equivalent circuit of an antenna with a connected transponder

WAVELYNX EX. 1008, Pg. 38
WaveLynx Technologies v. ASSA Abloy, IPR2023-00730

plane wave and a proportionality factor. The proportionality factor has the dimension of an area and is thus called the *effective aperture* A_e. The following applies:

$$P_e = A_e \cdot S \tag{4.75}$$

We can envisage A_e as an area at right angles to the direction of propagation, through which, at a given radiation density S, the power P_e passes (Meinke and Gundlach, 1992). The power that passes through the effective aperture is absorbed and transferred to the connected terminating impedance Z_T (Figure 4.64).

In addition to the effective aperture A_e, an antenna also possesses a *scatter aperture* $\sigma = A_s$ at which the electromagnetic waves are reflected.

In order to improve our understanding of this, let us once again consider Figure 4.63. When an electromagnetic field with radiation density S is received a voltage U_0 is induced in the antenna, which represents the cause of a current I through the antenna impedance Z_A and the terminating impedance Z_T. The current I is found from the quotient of the induced voltage U_0 and the series connection of the individual impedances (Kraus, 1988):

$$\mathrm{I} = \frac{\mathrm{U}_0}{\mathrm{Z}_\mathrm{T} + \mathrm{Z}_\mathrm{A}} = \frac{\mathrm{U}_0}{\sqrt{(\mathrm{R}_\mathrm{r} + \mathrm{R}_\mathrm{V} + \mathrm{R}_\mathrm{T})^2 + (\mathrm{X}_\mathrm{A} + \mathrm{X}_\mathrm{T})^2}} \tag{4.76}$$

Furthermore for the received power P_e transferred to Z_T:

$$P_e = I^2 \cdot R_T \tag{4.77}$$

Let us now substitute I^2 in equation (4.77) for the expression in equation (4.76), obtaining:

$$P_e = \frac{U_0^2 \cdot R_T}{(R_r + R_V + R_T)^2 + (X_A + X_T)^2} \tag{4.78}$$

According to equation (4.75) the effective aperture A_e is the quotient of the received power P_e and the radiation density S. This finally yields:

$$A_e = \frac{P_e}{S} = \frac{U_0^2 \cdot R_T}{S \cdot [(R_r + R_V + R_T)^2 + (X_A + X_T)^2]} \tag{4.79}$$

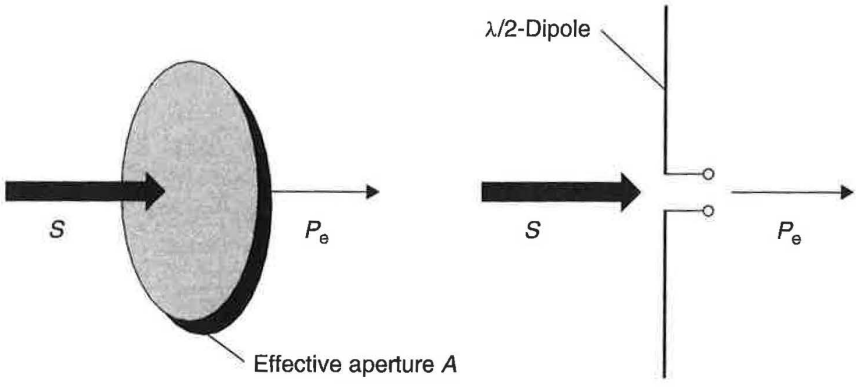


Figure 4.64 Relationship between the radiation density S and the received power P of an antenna

WAVELYNX EX. 1008, Pg. 39
WaveLynx Technologies v. ASSA Abloy, IPR2023-00730

If the antenna is operated using power matching, i.e. $R_T = R_V$ and $X_T = -X_A$, then the following simplification can be used:

$$A_e = \frac{{U_0}^2}{4SR_r} \tag{4.80}$$

As can be seen from Figure 4.63 the current I also flows through the radiation resistance R_r of the antenna. The converted power P_S is emitted from the antenna and it makes no difference whether the current I was caused by an incoming electromagnetic field or by supply from a transmitter. The power P_S emitted from the antenna, i.e. the reflected power in the received case, can be calculated from:

$$P_S = I^2 \cdot R_r \tag{4.81}$$

Like the derivation for equation (4.79), for the scatter aperture A_s we find:

$$\sigma = A_S = \frac{P_S}{S} = \frac{I^2 \cdot R_r}{S} = \frac{{U_0}^2 \cdot R_r}{S \cdot [(R_r + R_V + R_T)^2 + (X_A + X_T)^2]} \tag{4.82}$$

If the antenna is again operated using power matching and is also loss-free, i.e. $R_V = 0$, $R_T = R_r$ and $X_T = -X_A$, then as a simplification:

$$\sigma = A_S = \frac{U_0^2}{4SR_r} \tag{4.83}$$

Therefore, in the case of the power matched antenna $\sigma = A_s = A_e$. This means that only half of the total power drawn from the electromagnetic field is supplied to the terminating resistor R_T; the other half is reflected back into space by the antenna.

The behaviour of the scatter aperture A_s at different values of the terminating impedance Z_T is interesting. Of particular significance for RFID technology is the limit case $Z_T = 0$. This represents a short-circuit at the terminals of the antennas. From equation (4.82) this is found to be:

$$\sigma_{max} = A_{S\text{-}max} = \frac{{U_0}^2}{SR_r} = 4A_e|_{Z_T=0} \tag{4.84}$$

The opposite limit case consists of the connection of an infinitely high-ohmic terminating resistor to the antenna, i.e. $Z_T \to \infty$. From equation (4.82) it is easy to see that the scatter aperture A_s, just like the current I, tends towards zero.

$$\sigma_{min} = A_{S\text{-}min} = 0|_{Z_T \to \infty} \tag{4.85}$$

The scatter aperture can thus take on any desired value in the range 0–4 A_e at various values of the terminating impedance Z_T (Figure 4.65). This property of antennas is utilised for the data transmission from transponder to reader in backscatter RFID systems (see Section 4.2.6.6).

Equation (4.82) shows only the relationship between the scatter aperture A_S and the individual resistors of the equivalent circuit from Figure 4.63. However, if we are

WAVELYNX EX. 1008, Pg. 40
WaveLynx Technologies v. ASSA Abloy, IPR2023-00730

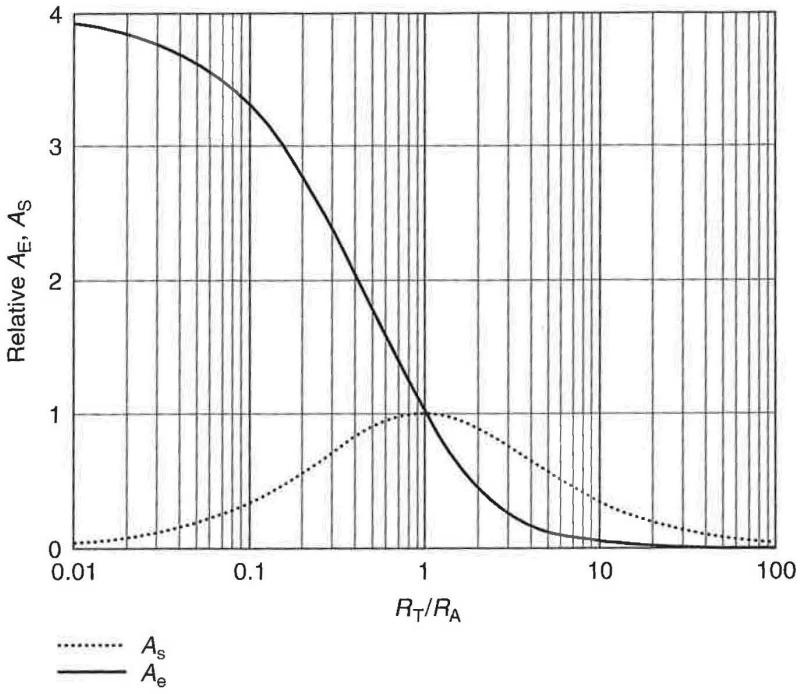


Figure 4.65 Graph of the relative effective aperture A_e and the relative scatter aperture σ in relation to the ratio of the resistances R_A and R_r. Where $R_T/R_A = 1$ the antenna is operated using power matching ($R_T = R_r$). The case $R_T/R_A = 0$ represents a short-circuit at the terminals of the antenna

to calculate the reflected power P_S of an antenna (see Section 4.2.4.1) we need the absolute value for A_S. The *effective aperture* A_e of an antenna is proportional to its gain G (Kraus, 1988; Meinke and Gundlach, 1992). Since the gain is known for most antenna designs, the effective aperture A_e, and thus also the scatter aperture A_S, is simple to calculate for the case of matching ($Z_A = Z_T$). The following is true[5]:

$$\sigma = A_e = \frac{\lambda_0^2}{4\pi} \cdot G \tag{4.86}$$

From equation (4.75) it thus follows that:

$$P_e = A_e \cdot S = \frac{\lambda_0^2}{4\pi} \cdot G \cdot S \tag{4.87}$$

4.2.5.5 Effective length

As we have seen, a voltage U_0 is induced in the antenna by an electromagnetic field. The voltage U_0 is proportional to the electric field strength E of the incoming wave.

[5] The derivation of this relationship is not important for the understanding of RFID systems, but can be found in Kraus (1988, chapter 2–22) if required.

WAVELYNX EX. 1008, Pg. 41
WaveLynx Technologies v. ASSA Abloy, IPR2023-00730

The proportionality factor has the dimension of a length and is therefore called the *effective length* l_0 (also *effective height* h) (Meinke and Gundlach, 1992). The following is true:

$$U_0 = l_0 \cdot E = l_0 \cdot \sqrt{S \cdot Z_F} \tag{4.88}$$

For the case of the matched antenna (i.e. $R_r = R_T$) the effective length can be calculated from the effective aperture A_e (Kraus, 1988):

$$l_0 = 2\sqrt{\frac{A_e \cdot R_r}{Z_F}} \tag{4.89}$$

If we substitute the expression in equation (4.86) for A_e, then the effective length of a matched antenna can be calculated from the gain G, which is normally known (or easy to find by measuring):

$$l_0 = \lambda_0\sqrt{\frac{G \cdot R_r}{\pi \cdot Z_F}} \tag{4.90}$$

4.2.5.6 Dipole antennas

In its simplest form the *dipole antenna* consists solely of a straight piece of line (e.g. a copper wire) of a defined length (Figure 4.66). By suitable shaping the characteristic properties, in particular the *radiation resistance* and bandwidth, can be influenced.

A simple, extended *half-wave dipole* ($\lambda/2$ dipole) consists of a piece of line of length $l = \lambda/2$, which is interrupted half way along. The dipole is supplied at this break-point (Figure 4.67).

The parallel connection of two $\lambda/2$ pieces of line a small distance apart ($d < 0.05\lambda$) creates the *2-wire folded dipole*. This has around four times the radiation resistance of

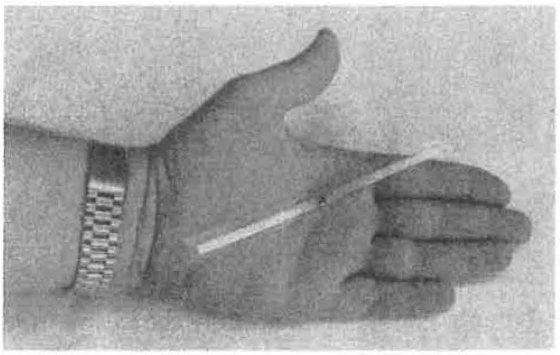


Figure 4.66 915 MHz transponder with a simple, extended dipole antenna. The transponder can be seen half way along (reproduced by permission of Trolleyscan, South Africa)

WAVELYNX EX. 1008, Pg. 42
WaveLynx Technologies v. ASSA Abloy, IPR2023-00730

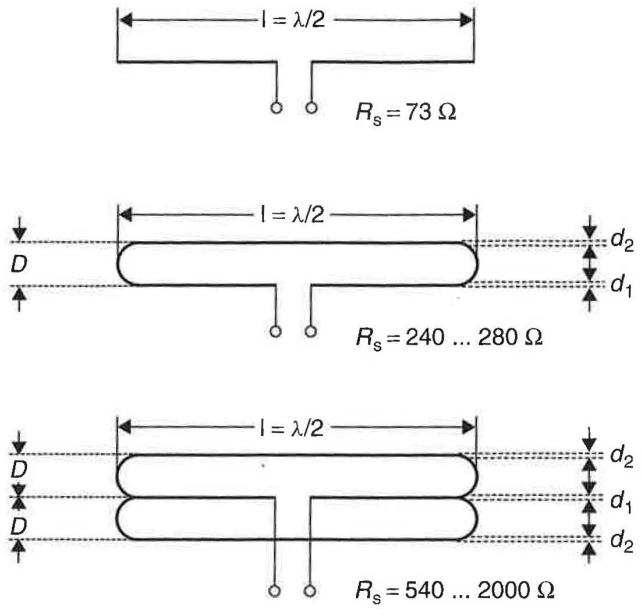


Figure 4.67 Different dipole antenna designs — from top to bottom: simple extended dipole, 2-wire folded dipole, 3-wire folded dipole

the single $\lambda/2$ dipole ($R_r = 240–280\,\Omega$). According to Rothammel (1981) the following relationship applies:

$$R_r = 73.2\,\Omega \cdot \left(\frac{\lg\left(\frac{4D^2}{d_1 \cdot d_2}\right)}{\lg\left(\frac{2D}{d_2}\right)} \right)^2 \tag{4.91}$$

A special variant of the loop dipole is the 3-wire folded dipole. The radiation resistance of the 3-wire folded dipole is greatly dependent upon the conductor diameter and the distance between the $\lambda/2$ line sections. In practice, the radiation resistance of the 3-wire folded dipole takes on values of 540–2000 Ω. According to Rothammel (1981) the following relationship applies:

$$R_r = 73.2\,\Omega \cdot \left(\frac{\lg\left(\frac{4D^3}{d_1^2 \cdot d_2}\right)}{\lg\left(\frac{D}{d_2}\right)} \right)^2 \tag{4.92}$$

The bandwidth of a dipole can be influenced by the ratio of the diameter of the $\lambda/2$ line section to its length, increasing as the diameter increases. However, the dipole must then be shortened somewhat in order to allow it to resonate at the desired frequency. In practice, the *shortening factor* is around 0.90–0.99. For a more precise calculation

WAVELYNX EX. 1008, Pg. 43
WaveLynx Technologies v. ASSA Abloy, IPR2023-00730

Table 4.8 Electrical properties of the dipole and 2-wire folded dipole

Parameter	Gain G	Effective aperture	Effective length	Apex angle
$\lambda/2$ dipole	1.64	$0.13\,\lambda^2$	$0.32\,\lambda$	78°
$\lambda/2$ 2-wire folded dipole	1.64	$0.13\,\lambda^2$	$0.64\,\lambda$	78°

of this topic, the reader is referred to the antenna literature, e.g. Rothammel (1981), Kraus (1988).

4.2.5.7 Yagi–Uda antenna

The *Yagi–Uda antenna*, named after its inventors, could well be the most important variant of a *directional antenna* in radio technology.

The antenna is an alignment array, made up of a driven emitter and a series of parasitic elements. A typical Yagi-Uda antenna is shown in Figure 4.68. Parasitic dipoles are arranged in front of the driven emitter (usually a dipole or 2-wire folded dipole) in the desired *direction of maximum radiation*. These parasitic dipoles function as *directors*, while a rod, usually a single rod, behind the exciter acts as a *reflector*. To create the directional transmission, the rods acting as directors must be shorter, and the rod acting as a reflector must be longer, than the exciter operating at resonance (Meinke and Gundlach, 1992). Compared to an isotropic emitter, gains of 9 dBi (based upon three elements) to 12 dB (based upon seven elements) can be achieved with a Yagi–Uda antenna. So-called 'long' Yagi antennas (10, 15 or more elements) can even achieve gains of up to 15 dBi in the main radiation direction.

Due to their size, Yagi–Uda antennas are used exclusively as antennas for readers. Like a torch, the Yagi–Uda antenna transmits in only one direction of maximum radiation, at a precisely known apex angle. Interference from adjacent devices or readers to the side can thus be suppressed and tuned out.

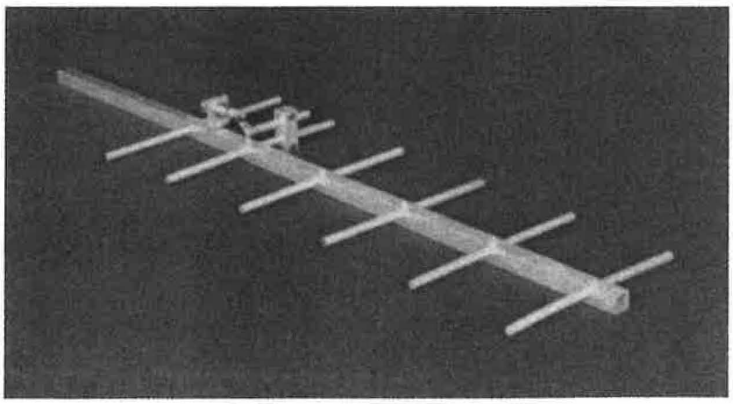


Figure 4.68 Typical design of a Yagi–Uda directional antenna (six elements), comprising a driven emitter (second transverse rod from left), a reflector (first transverse rod from left) and four directors (third to sixth transverse rods from left) (reproduced by permission of Trolleyscan, South Africa)

WAVELYNX EX. 1008, Pg. 44
WaveLynx Technologies v. ASSA Abloy, IPR2023-00730

Due to the popularity of the Yagi–Uda antenna both as an antenna for radio and television reception and also in commercial radio technology, there is a huge amount of literature on the operation and construction of this antenna design. Therefore, we will not deal with this antenna in more detail at this point.

4.2.5.8 Patch or microstrip antenna

Patch antennas (also known as *microstrip* or *planar antennas*) can be found in many modern communication devices. For example, they are used in the latest generations of GPS receivers and mobile telephones, which are becoming smaller all the time. Thanks to their special construction format, patch antennas also offer some advantages for RFID systems.

In its simplest form, a patch antenna comprises a printed circuit board (e.g. Teflon or PTFE for higher frequencies) coated (i.e. metallised) on both sides, the underside of which forms a continuous ground (Kraus, 2000). On the top there is a small rectangle, which is supplied via a microstrip feed on one side, feeders through the base plate (see Figure 4.71) or capacitive coupling via an intermediate layer (aperture coupled patch antenna; see Kossel (n.d.), Fries and Kossel (n.d.)). Planar antennas can therefore be manufactured cheaply and with high levels of reproducibility using PCB etching technology (see Figures 4.69 and 4.70).

The length L_p of the patch determines the resonant frequency of the antenna. Under the condition $h_D \leq \lambda$:

$$L_P = \frac{\lambda}{2} - h_D \tag{4.93}$$

Normally the substrate thickness h_D is 1–2% of the wavelength.

The width w_p influences the resonant frequency of the antenna only slightly, but determines the *radiation resistance* R_r of the antenna (Krug, 1985). Where $w_p < \lambda/2$:

$$R_r = \frac{90}{\frac{\varepsilon_r + 1}{2} + (\varepsilon_r - 1)\sqrt{4 + \frac{48 \cdot h_p}{w_p}}} \cdot \left(\frac{\lambda}{w_p}\right)^2 \tag{4.94}$$

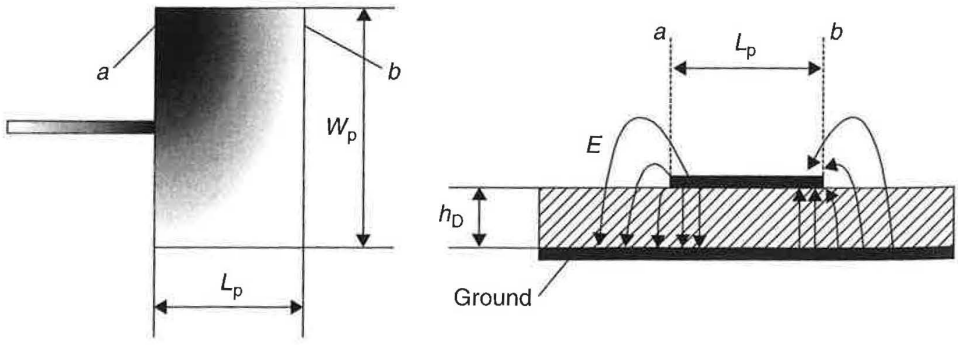


Figure 4.69 Fundamental layout of a patch antenna. The ratio of L_p to h_D is not shown to scale

WAVELYNX EX. 1008, Pg. 45
WaveLynx Technologies v. ASSA Abloy, IPR2023-00730

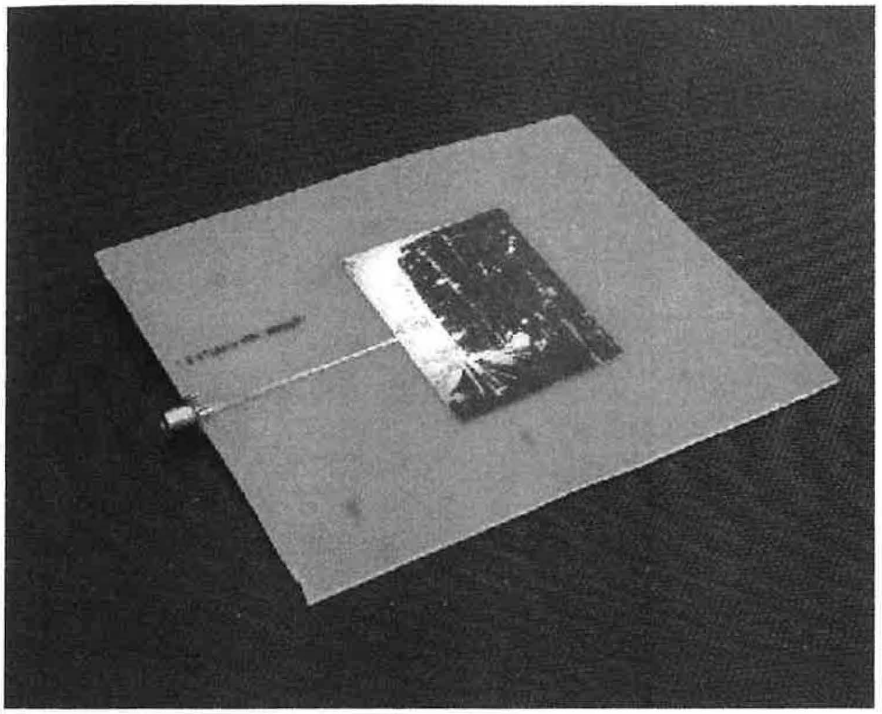


Figure 4.70 Practical layout of a patch antenna for 915 MHz on a printed circuit board made of epoxy resin (reproduced by permission of Trolleyscan, South Africa)

where $w_p > 3\lambda/2$:

$$R_r = \frac{120}{\frac{\varepsilon_r + 1}{2} + (\varepsilon_r - 1)\sqrt{4 + \frac{48 \cdot h_p}{w_p}}} \cdot \frac{\lambda}{w_p} \tag{4.95}$$

If the patch antenna is operated at its resonant frequency the phase difference between the patch edges a and b is precisely 180°. Figure 4.69 shows the path of the electrical field lines. At the entry and exit edges of the patch the field lines run in phase. The patch edges a and b thus behave like two in-phase fed slot antennas. The polarisation of the antenna is linear and parallel to the longitudinal edge L_p. See Figure 4.71.

Due to the type of power supply, patch antennas can also be used with *circular polarisation*. To generate circular polarisation, an emitter element must be supplied with signals with a phase angle of 90° at only two edges that are geometrically offset by 90°.

It is a relatively simple matter to amalgamate patch antennas to form *group antennas* (Figure 4.72). As a result, the gain increases in relation to that of an individual element. The layout shown in the figure comprises in-phase fed emitter elements. The approximately $\lambda/2$ long patch elements are fed via almost non-radiative line sections of around $\lambda/2$ in length connected in series, so that the transverse edges a–a or b–b of the patch element lie precisely wavelength λ apart. Thus the in-phase feed to the

WAVELYNX EX. 1008, Pg. 46
WaveLynx Technologies v. ASSA Abloy, IPR2023-00730

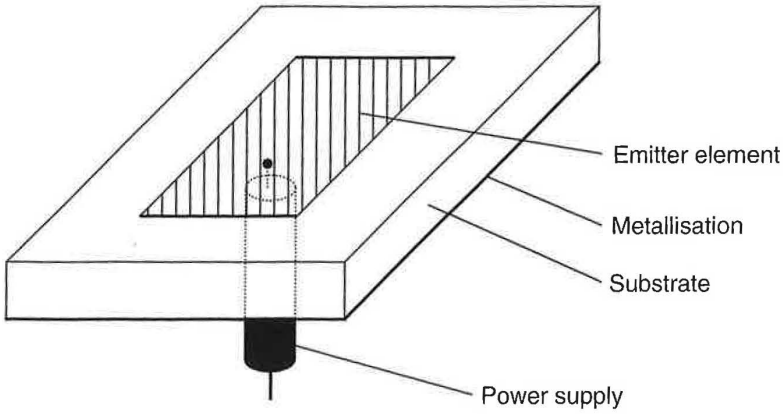


Figure 4.71 Supply of a $\lambda/2$ emitter quad of a patch antenna via the supply line on the reverse

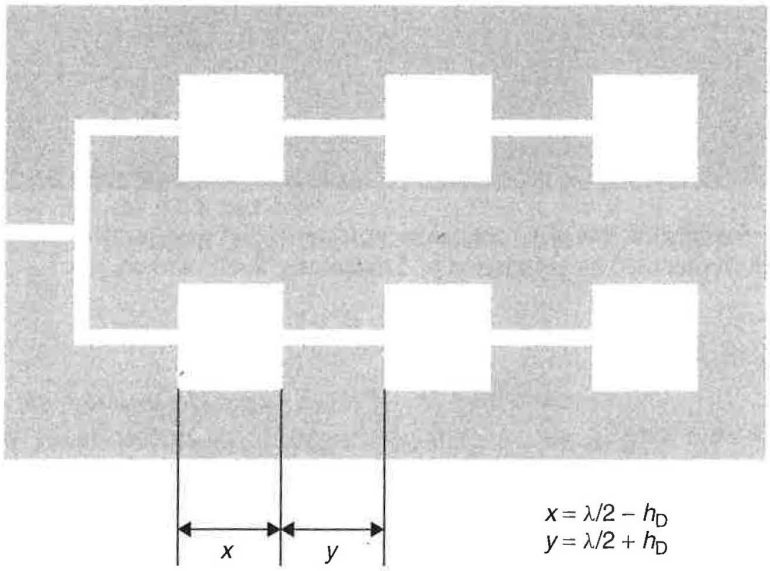


Figure 4.72 The interconnection of patch elements to form a group increases the directional effect and gain of the antenna

individual elements is guaranteed. The arrangement is polarised in the direction of the line sections.

4.2.5.9 Slot antennas

If we cut a strip of length $\lambda/2$ out of the centre of a large metal surface the slot can be used as an emitter (Rothammel, 1981). The width of the slot must be small in relation to its length. The base point of the emitter is located at the mid-point of its longitudinal side (Figure 4.73).

WAVELYNX EX. 1008, Pg. 47
WaveLynx Technologies v. ASSA Abloy, IPR2023-00730

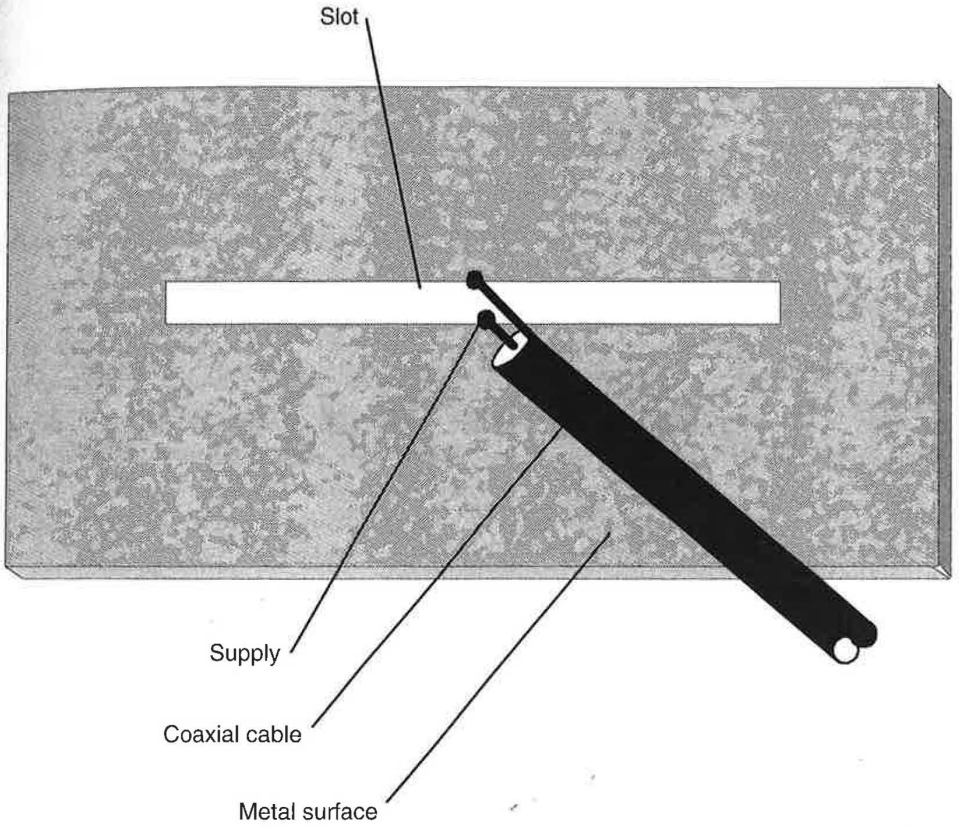


Figure 4.73 Layout of a slot antenna for the UHF and microwave range

4.2.6 Practical operation of microwave transponders

Let us now turn our attention to practical operation when a transponder is located in the *interrogation zone* of a reader. Figure 4.74 shows the simplified model of such a *backscatter system.* The reader emits an electromagnetic wave with the effective radiated power $P_1 \cdot G_1$ into the surrounding space. Of this, a transponder receives power $P_2 = P_e$, proportional to the field strength E, at distance r.

Power P_S is also reflected by the transponder's antenna, of which power P_3 is again received by the reader at distance r.

4.2.6.1 Equivalent circuits of the transponder

In the previous sections we have quoted the simplified equation for the impedance of the transformer $Z_T = R_T + jX_T$ (simplified equivalent circuit). In practice, however, the *input impedance* of a transponder can be represented more clearly in the form of the parallel circuit consisting of a *load resistor* R_L, an *input capacitor* C_2, and possibly a modulation impedance Z_{mod} (see also Section 4.2.6.6) (functional equivalent circuit).

WAVELYNX EX. 1008, Pg. 48
WaveLynx Technologies v. ASSA Abloy, IPR2023-00730

5

Frequency Ranges and Radio Licensing Regulations

5.1 Frequency Ranges Used

Because RFID systems generate and radiate electromagnetic waves, they are legally classified as *radio systems*. The function of other *radio services* must under no circumstances be disrupted or impaired by the operation of RFID systems. It is particularly important to ensure that RFID systems do not interfere with nearby radio and television, mobile radio services (police, security services, industry), marine and aeronautical radio services and mobile telephones.

The need to exercise care with regard to other radio services significantly restricts the range of suitable operating frequencies available to an RFID system (Figure 5.1). For this reason, it is usually only possible to use frequency ranges that have been reserved specifically for industrial, scientific or medical applications. These are the frequencies classified worldwide as *ISM frequency ranges* (Industrial–Scientific–Medical), and they can also be used for RFID applications.

In addition to ISM frequencies, the entire *frequency range* below 135 kHz (in North and South America and Japan: <400 kHz) is also suitable, because it is possible to work with high magnetic field strengths in this range, particularly when operating inductively coupled RFID systems.

The most important frequency ranges for RFID systems are therefore 0–135 kHz, and the ISM frequencies around 6.78 (not yet available in Germany), 13.56 MHz, 27.125 MHz, 40.68 MHz, 433.92 MHz, 869.0 MHz, 915.0 MHz (not in Europe), 2.45 GHz, 5.8 GHz and 24.125 GHz.

An overview of the estimated distribution of RFID transponders at the various *frequencies* is shown in Figure 5.2.

5.1.1 Frequency range 9–135 kHz

The range below 135 kHz is heavily used by other radio services because it has not been reserved as an ISM frequency range. The propagation conditions in this *long wave*

RFID Handbook: Fundamentals and Applications in Contactless Smart Cards and Identification. Klaus Finkenzeller
© 2003 John Wiley & Sons, Ltd ISBN: 0-470-84402-7

WAVELYNX EX. 1008, Pg. 49
WaveLynx Technologies v. ASSA Abloy, IPR2023-00730

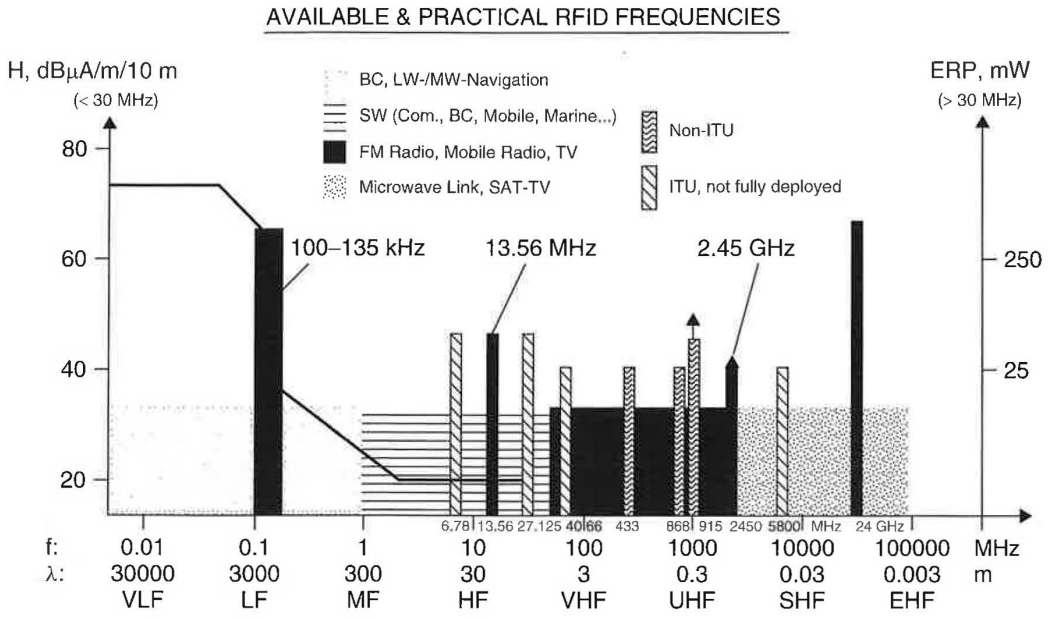


Figure 5.1 The frequency ranges used for RFID systems range from the myriametric range below 135 kHz, through short wave and ultrashort wave to the microwave range, with the highest frequency being 24 GHz. In the frequency range above 135 kHz the ISM bands available worldwide are preferred

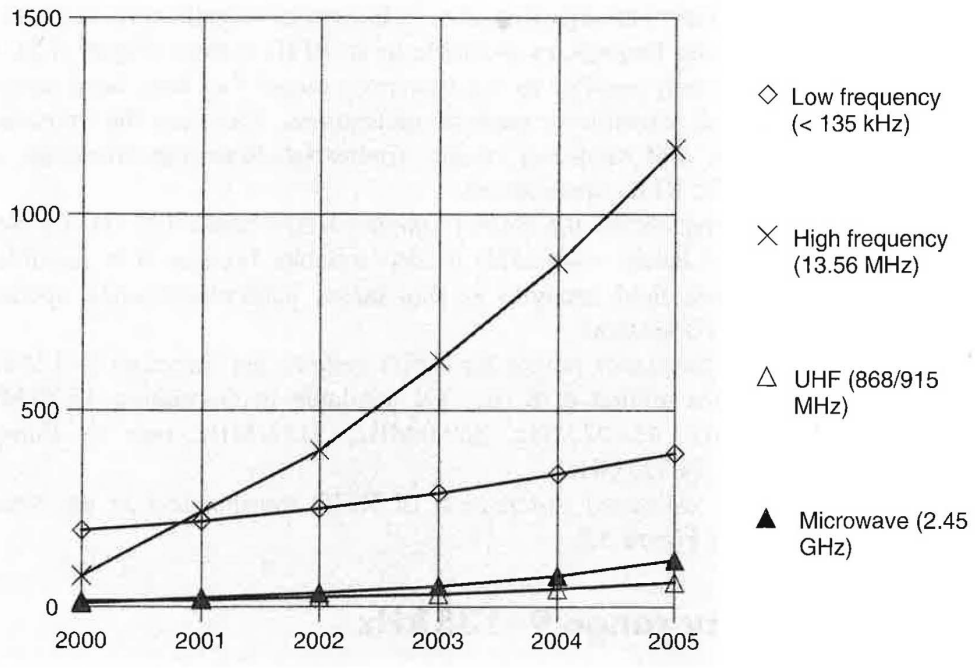


Figure 5.2 The estimated distribution of the global market for transponders over the various frequency ranges in million transponder units (Krebs, n.d.)

WAVELYNX EX. 1008, Pg. 50
WaveLynx Technologies v. ASSA Abloy, IPR2023-00730